Hypocentre determination offshore Eastern Taiwan using the Maximum Intersection method

Y. Font, Honn Kao, S. Lallemand, Char-Shine Liu, Ling-Yun Chiao

▶ **To cite this version:**

Y. Font, Honn Kao, S. Lallemand, Char-Shine Liu, Ling-Yun Chiao. Hypocentre determination offshore Eastern Taiwan using the Maximum Intersection method. Geophysical Journal International, 2004, 158 (2), pp.655-675. 10.1111/j.1365-246X.2004.02317.x . hal-00407311

HAL Id: hal-00407311
https://hal.science/hal-00407311

Submitted on 1 Feb 2021

HAL is a multi-disciplinary open access archive for the deposit and dissemination of scientific research documents, whether they are published or not. The documents may come from teaching and research institutions in France or abroad, or from public or private research centers.

L'archive ouverte pluridisciplinaire **HAL**, est destinée au dépôt et à la diffusion de documents scientifiques de niveau recherche, publiés ou non, émanant des établissements d'enseignement et de recherche français ou étrangers, des laboratoires publics ou privés.

Geophys. J. Int. (2004) **158,** 655–675 doi: 10.1111/j.1365-246X.2004.02317.x

Hypocentre determination offshore of eastern Taiwan using the Maximum Intersection method

Yvonne Font,[1] Honn Kao,[2] Serge Lallemand,[3] Char-Shine Liu[4] and Ling-Yun Chiao[4]

[1] *Géosciences Azur, Obs. Océanologique Villefranche,* B.P. 48, 06235, *Villefranche sur Mer, France*
[2] *Pacific Geoscience Center, Geological Survey of Canada,* PO Box 6000, *Sidney,* BC V8L 4B2, *Canada*
[3] *Lab. DL, Université de Montpellier* 2, *Montpellier, France*
[4] *Institute of Oceanography, National Taiwan University, Taipei, Taiwan*

Accepted 2004 March 23. Received 2004 March 19; in original form 2003 March 3

Downloaded from https://academic.oup.com/gji/article/158/2/655/771828 by guest on 01 February 2021

SUMMARY

The maximum intersection (MAXI) method, which derives from the master station method (MSM), determines within a 3-D velocity model the absolute hypocentral location based on observed arrival times. First, the spatial node that better satisfies the arrival time differences computed at all station pairs, plus or minus an error tolerance value (in seconds), is defined as the preliminary hypocentral solution (PRED). Second, because PRED depends neither on the estimate of origin time nor on the residual root mean square (rms), residual outliers are objectively detected and cleaned out from the original data set without any iterative process or weighting. Third, a statistical minimization (residual rms) is conducted in a small domain around the PRED node, which results in a unique FINAL solution. The MAXI method is applied to the determination of earthquake hypocentres (with the proper station correction terms) in the southernmost extremity of the Ryukyu subduction zone, where several dense seismic clusters occur near the seismogenic plate interface. The location of earthquakes, recorded at both the Taiwanese and Japanese networks, is obtained for about a thousand events (between 1992 and 1997). The process uses a detailed 3-D velocity model based on multiple geophysical data sources obtained in the junction area between subduction and collision (east of Taiwan). The earthquake clustering and the significant drop in residual statistics (1.20, 0.80 and 0.35 s, for Taiwanese catalogue, MSM and MAXIM solutions respectively) indicate the accuracy of the method, which can be used to routinely determine absolute hypocentre location based on observed arrival times.

Key words: 3-D, earthquake, hypocentre, location, outlier, Taiwan.

INTRODUCTION

Determination of the location of seismic events is one of the most fundamental problems in seismology as well as in tectonic investigations because inaccuracies in earthquake location often lead to controversy. The routine determinations of local seismicity catalogues, for reasons of promptness and consistency with prior determinations, are usually performed using iterative methods that aim to minimize traveltime residues (observed minus computed travel time) within a standard velocity model (e.g. HYPO71 (Lee & Lahr 1975) or FASThypo (Herrman 1979)). Those methodologies are indeed fast, but often the precision of the hypocentral solutions does not allow tectonic interpretations. The location errors are linked to the velocity model that usually poorly represents the complex geological structures in seismogenic zones, the configuration of the seismic network (especially for offshore earthquakes), the techniques that are used to trace the seismic rays and the methodologies that determine the hypocentres. However, during the last 20 yr great progress has been made in hypocentral location research, largely supported by improvements in computer capabilities, seismic networks and recording quality, but these improved methods are generally not taken into consideration in determining routine catalogues.

For example, modern 3-D hypocentral location methods are strongly dependent on 3-D velocity models (e.g. Wittlinger *et al.* 1993; Zhou 1994; Lomax *et al.* 2000). These refined 3-D models are obtained thanks to advances made in joint hypocentre–velocity codes (e.g. Pavlis & Booker 1980; Thurber 1983). Progress in relative location (even though 1-D layered models are often used) greatly increases the accuracy of the relative location of similar events within seismic clusters (e.g. Jordan & Sverdrup 1981; Smith 1982; Pujol 1988, 1992, 1995; Waldhausser & Ellsworth 2000), whether or not waveform correlation techniques are used (e.g. Got *et al.* 1994; Poupinet *et al.* 1984; Rubin & Gillard 2000). However, knowledge about precise event offsets between earthquake hypocentres is often insufficient to solve tectonic problems if the absolute location of the cluster is unknown.

© 2004 RAS

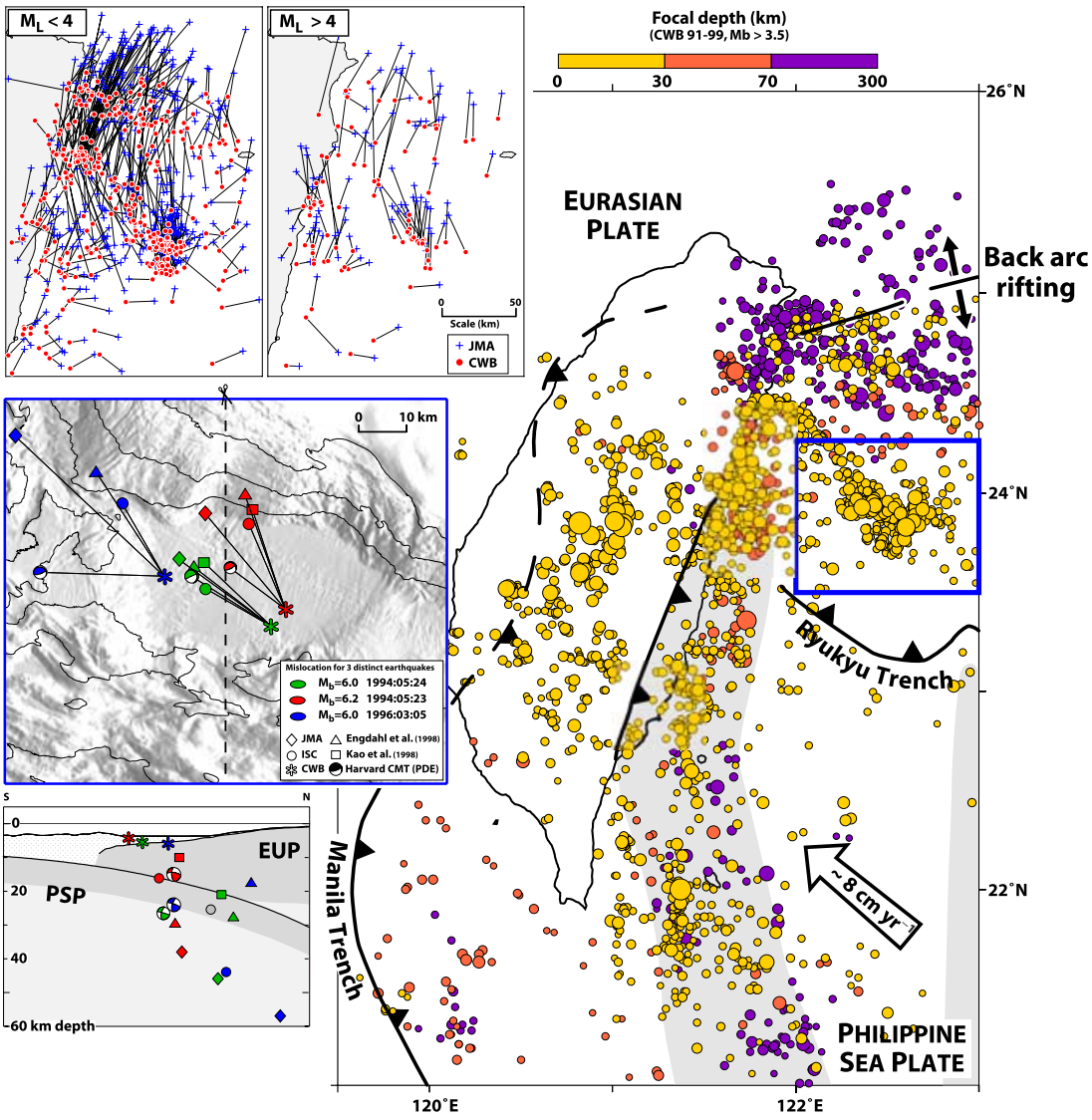

Figure 1. Seismicity in the Taiwan area and geodynamic context (relative convergence is after Yu *et al.* 1997) for earthquakes which occurred between 1991 and 1999 ($M_b > 3.5$) from the local catalogue of the Central Weather Bureau of Taiwan (CWB). The grey domains represent the Luzon volcanic arc to the west and the Gagua Ridge to the east. Upper left: location comparison between CWB and Japanese Meteorological Agency (JMA) determinations. Centre and lower left: comparison between different determinations of three events with M_b greater than 6, on map view and vertical cross-section (ISC, International Seismological Center; PDE, preliminary determination epicentre).

Offshore of eastern Taiwan, the 3-D earth model is intricate because of the interactions between the westernmost extremity of the Ryukyu subduction slab and the arc–continent collision system (e.g. Lallemand *et al.* 1997b; Font *et al.* 1999; Font 2001). Several dense seismic swarms prevail at shallow to intermediate depths in the vicinity of the seismogenic plate interface, along the backarc basin or at the site of active collision. Earthquake distribution is more scattered within the Philippine Sea Plate oceanic basin, south of the Ryukyu Trench (Fig. 1). Despite the tectonic importance of the area, previously reported hypocentral determinations are associated with large location uncertainties. The local routine hypocentre catalogue from the Central Weather Bureau of Taiwan (CWB) proceeds from an iterative least-squares approach, HYPO71 (Lee & Lahr 1975), using a flat-layered velocity model (Chen & Shin 1998), which results in poor location accuracy in the offshore domain (on average root mean square (rms) residual errors reach 1.25 s). For seismic events of M_L larger than 6.0, hypocentres from CWB show a location discrepancy greater than 30 km compared with global data sets (ISC or PDE from the USGS NEIC) or with relocation works based on teleseismic data (Engdahl *et al.* 1998; Kao *et al.* 1998). Compared with local determinations from the Japanese Meteorological Agency (JMA), the horizontal location differences attain an average of 60 km for earthquakes of M_L less than 4.0. Consequently, seismotectonic interpretations differ widely in the area depending on which hypocentre data set is referred to and significant controversies still exist concerning the geometry of the active systems (e.g. Hsu & Sibuet 1995; Chemenda *et al.* 1997; Kao *et al.* 1998; Font *et al.* 1999; Lallemand *et al.* 1997b; Sibuet & Hsu 1997).

In this paper we present the maximum intersection (MAXI) method applied to the absolute location of local earthquakes occurring offshore of eastern Taiwan. This new method is based on

Downloaded from https://academic.oup.com/gji/article/158/2/655/771828 by guest on 01 February 2021

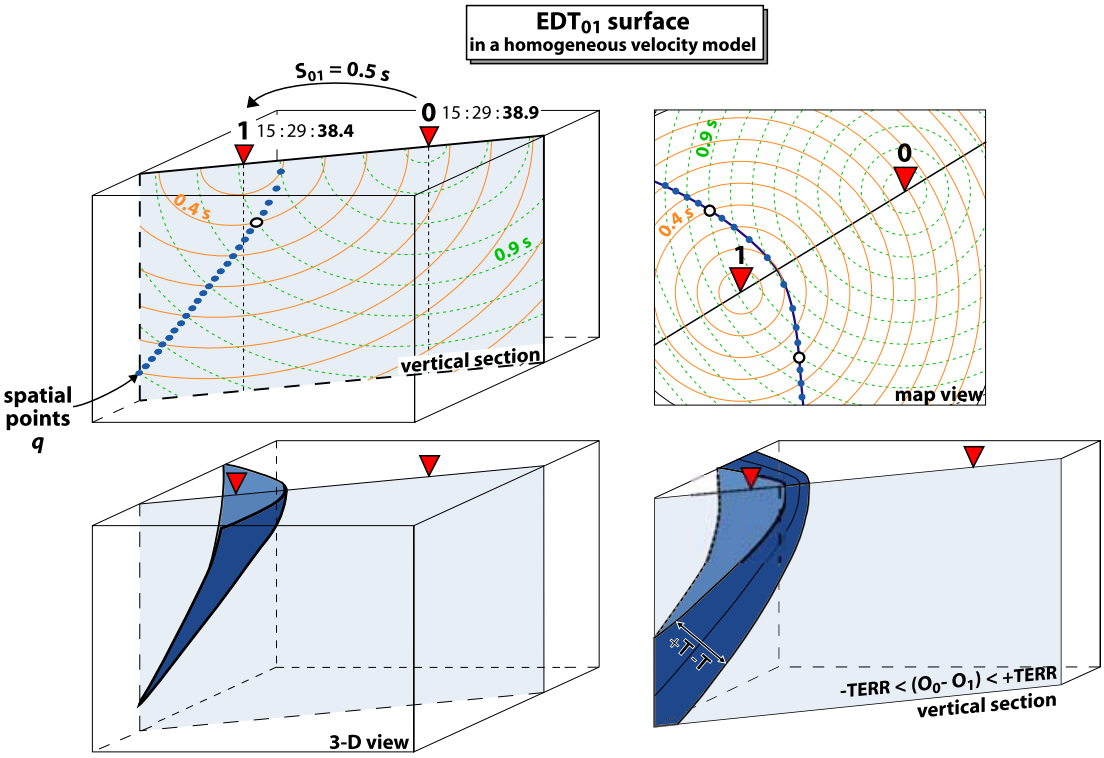

Figure 2. Illustration of an equal differential time (EDT) surface in a homogeneous velocity model. Upper left: collection of spatial points satisfying an arrival time difference of 0.5 s at the two stations 0 and 1, presented on a vertical section. Upper right: collection of spatial points on the map view. Lower left: schematization of the EDT surface on a 3-D view. Lower right: illustration of the TERR parameter (T) on a vertical section.

the master station method (MSM) (Zhou 1994), which has been improved to solve particular problems encountered in this study.

The MSM (Zhou 1994) is well adapted for investigations based on local seismic data because it uses 3-D earth models presenting strong lateral heterogeneities. The MSM algorithm seeks the absolute location of each earthquake independently by using equal difference time (EDT) surfaces established from *P*-wave measurement differences at pairs of stations (Fig. 2). The pairs of stations lumped together during the process (and their associated EDT surfaces) correspond to all couples of stations combined with a single 'reference station', St_0, which is the *nearest* (in time) station from the hypocentre. The MSM algorithm has already demonstrated its efficiency and robustness in dense seismic networks with good quality recordings, for example in California (Zhou 1994) and Taiwan (on land) (Kao *et al.* 2000).

Offshore of eastern Taiwan, due to insufficient seismic ray path coverage and the lack of seismic stations on the east of the island, seismic tomography cannot be well constrained in our study area, especially in depth (Hsu 2001). To start, we thus construct the first comprehensive 3-D velocity model to strengthen our hypocentral determination process (Font 2001; Font *et al.* 2003). Second, we improve the azimuthal coverage of offshore earthquakes by combining the four nearest Japanese seismic stations to the Taiwanese ones. And third, because of the inconsistency in seismic data quality (most probably originating from the associated large source–station distances and/or the combination of the two independent network data), we have been led to modify the MSM. As a matter of fact, the reference station St_0 is, in many cases for the eastern Taiwan study, distant by at least 80 km from the densest swarm and has occasionally shown biased records. Because the performance of the MSM is controlled by the accuracy of the reference station arrival time measurement, such records have dramatic effects onto the relocation process; thus it has been necessary to adapt the algorithm to confront this issue. Consequently, we have developed the MAXI method, which is an improved version of the MSM. In the following we will restate the main concepts of EDT surfaces, describe the MAXI algorithm and explain, among other characteristics, how the method avoids computing residual minimums during the preliminary determination of the hypocentre. As a result of this preliminary procedure, thanks to a statistical basis that contrasts from the usual L1 or L2 norms, we can objectively decontaminate non-systematic residual outliers from an original set of *P* arrivals. Distinct 3-D hypocentral procedures, from the MSM to the MAXI algorithm, are tested and the resulting earthquake locations establish the robustness of the method. The clustering and alignment of hypocentres relocated independently of each other shows an improvement in earthquake location in northeastern Taiwan.

THE MAXI METHOD

The MAXI algorithm is developed based on the MSM first presented by (Zhou 1994). This section aims to describe the performance of the improved method and readers are referred to Zhou (1994) for more details about the original method. We will first recall the concept of EDT surfaces and then explain the MAXI method.

Equal differential time surface

Theoretically, if a hypocentre r is perfectly determined within the earth model, then the difference between the traveltimes C_{rj} and C_{rk} computed at two seismic stations j and k should be equal to the

Downloaded from https://academic.oup.com/gji/article/158/2/655/771828 by guest on 01 February 2021

difference between the two observed traveltimes tt_{rj} and tt_{rk}.

$$tt_{rj} - tt_{rk} = C_{rj} - C_{rk} \quad (1)$$

Because an observed traveltime corresponds to the difference between the measured arrival time and the estimated origin time of the earthquake, the difference between the two traveltimes computed at stations j and k is equal to the difference between the corresponding observed arrival times, O_{rj} and O_{rk}:

$$O_{rj} - O_{rk} = C_{rj} - C_{rk} \quad (2)$$

In other words, the hypocentre occurs on a spatial surface S_{jk} defined by a variable point q, which satisfies

$$S_{jk} = O_j - O_k = C_{qj} - C_{qk} \quad (3)$$

where C_{qj} and C_{qk} are the computed traveltimes from the spatial point q to the two stations j and k, in the velocity model (Fig. 2). S_{jk} is the mathematical expression of the EDT surface between the stations j and k.

Therefore, an EDT surface is defined as the collection of all spatial points within the velocity model that satisfy the time difference between the arrivals observed at two stations. In a homogeneous velocity model, this surface corresponds to a 3-D hyperbolic surface with its horizontal symmetry axis going through the two stations. In heterogeneous velocities, the EDT surface is a deformed hyperbolic surface. Note that the collection of spatial points that define an EDT surface is established from (1) the difference between observed traveltimes and (2) the ray path computation from one grid node to the seismic station, within the velocity model. Consequently, by definition, an EDT surface is independent not only of the estimate of the time of origin of the earthquake but also of residuals and any type of residual statistics (L1, L2 norms).

Furthermore, because the construction of the EDT surface refers to two arrival readings, the noise level of a surface is comparable to that of observed traveltimes (Zhou 1994). To include this noise level and small picking errors, the EDT surface is thickened by a tolerance error value, called TERR. Thus, the collection of spatial points will in fact account for the computed time difference plus or minus the TERR value, and consequently what we called an 'EDT surface' is, in fact, a narrow volume (Fig. 2). Following Zhou (1994) and Kao *et al.* (2000), an appropriate value for TERR is 0.5 s.

The MAXI method

The MAXI method constrains the hypocentre by searching the node within the velocity model that satisfies two types of criteria (Figs 3b and d). The first criterion is that the node is traversed by the maximum number of EDT surfaces. The second criterion fixes the FINAL solution by minimizing residual statistics. For reasons of data contamination, another step is required prior to searching for the statistical minimum: cleaning outlier(s) from the original set of data (Fig. 3c).

Pre-determination step

In our investigation, the concept of EDT surface is generalized to the case of a single phase (P phase) observed at all the J seismic stations $(0, 1, 2, \ldots, J-1)$ that constitute the network (Fig. 3a). Relative to the station called 0, a set of $J-1$ independent EDT surfaces $S_{01}, S_{02}, S_{03} \ldots S_{0(J-1)}$ can be constructed. To avoid any dependence with a single arrival time (e.g. with the station 0 or reference station), we increase to the maximum the number of observations by combining all station pairs available. For J seismic stations, the total number of EDT surfaces involved in the process is:

$$C_2^J = \frac{J(J-1)}{2} \quad (4)$$

During the pre-determination step, the spatial point intersected by the maximum number of EDT surfaces, among the whole set of surfaces involved in the process (Fig. 3b), is defined as the preliminary hypocentre solution (PRED). Because our studied area is mostly located below sea level, the algorithm forbids this spatial point to be situated within the water or in soft sediments.

As a consequence of the thickness TERR allowed for each surface, the intersection of EDT surfaces defines a small volume where it may happen that several spatial points are crossed by the same maximum number of EDT surfaces. Given the set of P arrivals and the TERR boxcar shape, those candidates have *a priori* the same probability of representing the hypocentre, and usually they are only a few kilometres distant from each other.

Outlier cleaning step

The delineation of the EDT surface involves statistics that differ widely from residual statistics (L1 or L2 norms). Therefore, the PRED solution, defined by the intersection of EDT surfaces, is determined by the probability of the arrival time data set to resolve the unknown hypocentral parameters. Consequently, one advantage of the MAXI algorithm is to objectively detect and clean out outliers that may exist in the original data set. In the following, we first explain how an outlier corrupts a classical residual minimization process. We then specify how the MAXI method detects those outliers and avoids contamination by them.

Effects of outlier(s) on a traditional residual minimization process

Most of the classical earthquake location techniques minimize residual statistics to seek the best hypocentral solution. Those techniques often examine an L2 norm such as the variance rms (e.g. eq. 5) applied to the statistical population of traveltime residues:

$$V(r) = \sum_{j=0}^{J-1} (tt_j - C_j)^2 \quad (5)$$

For a hypocentral determination, the residual rms value is indicative of the distribution, or spreading, of the residues with respect to their average (e.g, Fig. 4). The rms factor therefore conveys the notion of 'certainty', as the lower the rms value the more the traveltime residues are distributed closely to their average and the more the computed traveltimes seem to properly reflect the *observed* traveltime. In such a case we tend to think that the earthquake determination approaches the hypocentre. But a low rms does not always indicate a good determination. Imagine, for example, a perfect case where a determination is perfectly located at the real hypocentre, in a velocity model that exactly reflects the earth structure, but with a set of P arrival times that contains an incorrect arrival measurement. In such a case, all traveltime residues should equal zero except for one spurious residue that incontestably increases the rms value. Consequently, even though the hypocentral determination is perfectly located, the relatively high rms does not reflect the accuracy of the location. In real applications, we don't know *a priori* if outliers exist in the set of residues. When they do exist, the statistical search by minimization will obviously find a solution that best minimizes the residues, with a lower rms value than

Downloaded from https://academic.oup.com/gji/article/158/2/655/771828 by guest on 01 February 2021

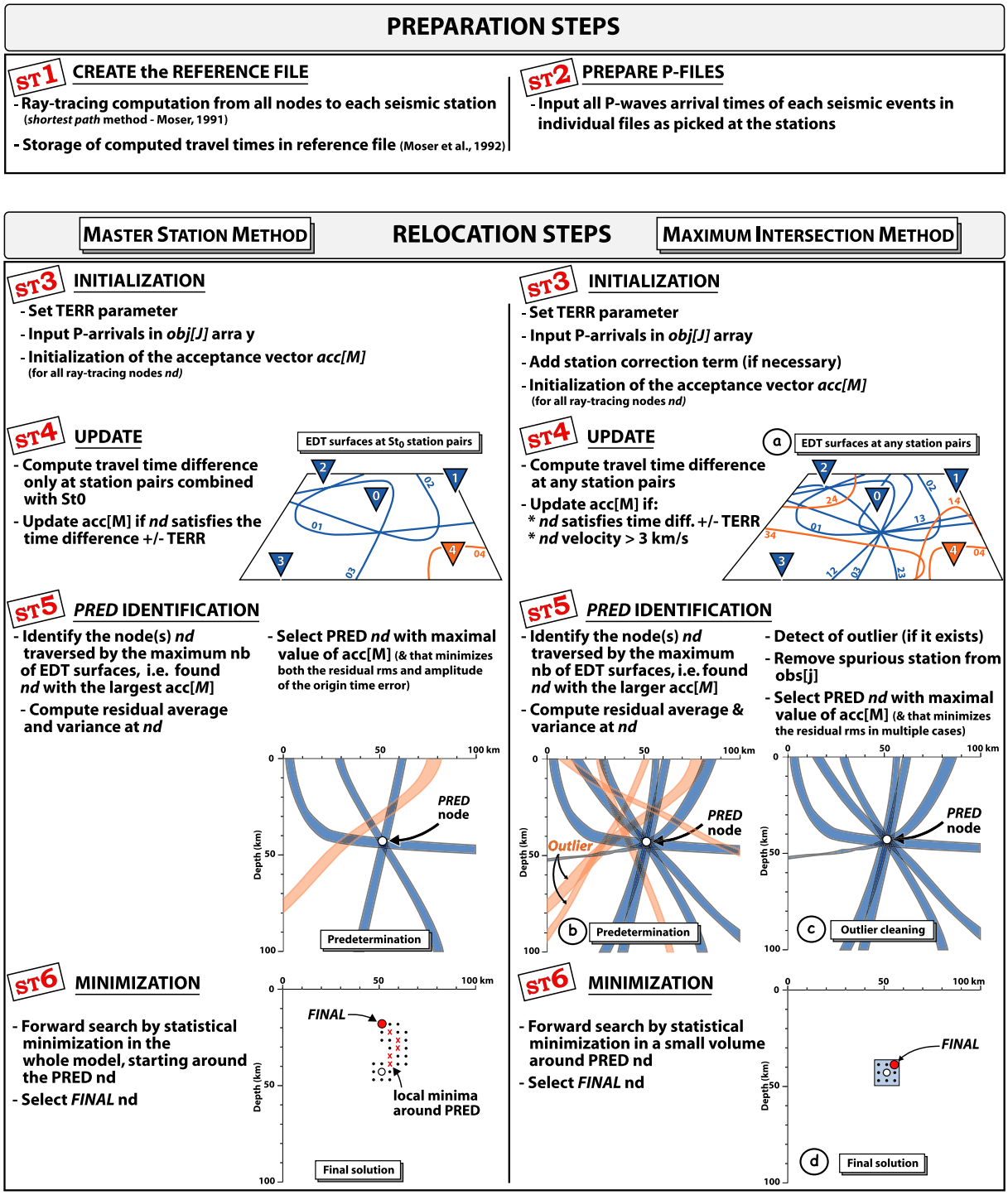

Figure 3. Schematization of the MAXI method procedure in a network of $J = 5$ seismic stations compared with the MSM (Zhou 1994). (a) Example of intersection of the $[J(J-1)]/2 = 10$ EDT surfaces on a map view, with one spurious measurement in the set of P arrivals (at station 4). Note that the EDT thickness (TERR) is not represented in this view. (b) First step of the procedure: determination of the node (PRED) intersected by the maximum number of EDT surfaces on a vertical section, with a series of incongruent EDT surfaces (associated with the station 4 spurious measurement). The diagram aims to schematize how an incongruent EDT surface will not affect the determination of PRED. (c) Second step of the MAXI procedure: outlier cleaning. (d) Third step of the procedure: search for the FINAL solution that minimizes residual statistics in a restricted domain surrounding PRED (see text for further details).

the one computed at the hypocentre location. The process therefore results in an inaccurate hypocentre solution that nevertheless will be qualified by a low rms—or at least, lower than the one associated with the exact hypocentre location. It is therefore necessary to detect outliers without using a minimization process. In applications with real data, for a single earthquake with data including one outlier, we have observed that the distance between two solutions determined by residual minimization, on the one hand, and by

Downloaded from https://academic.oup.com/gji/article/158/2/655/771828 by guest on 01 February 2021

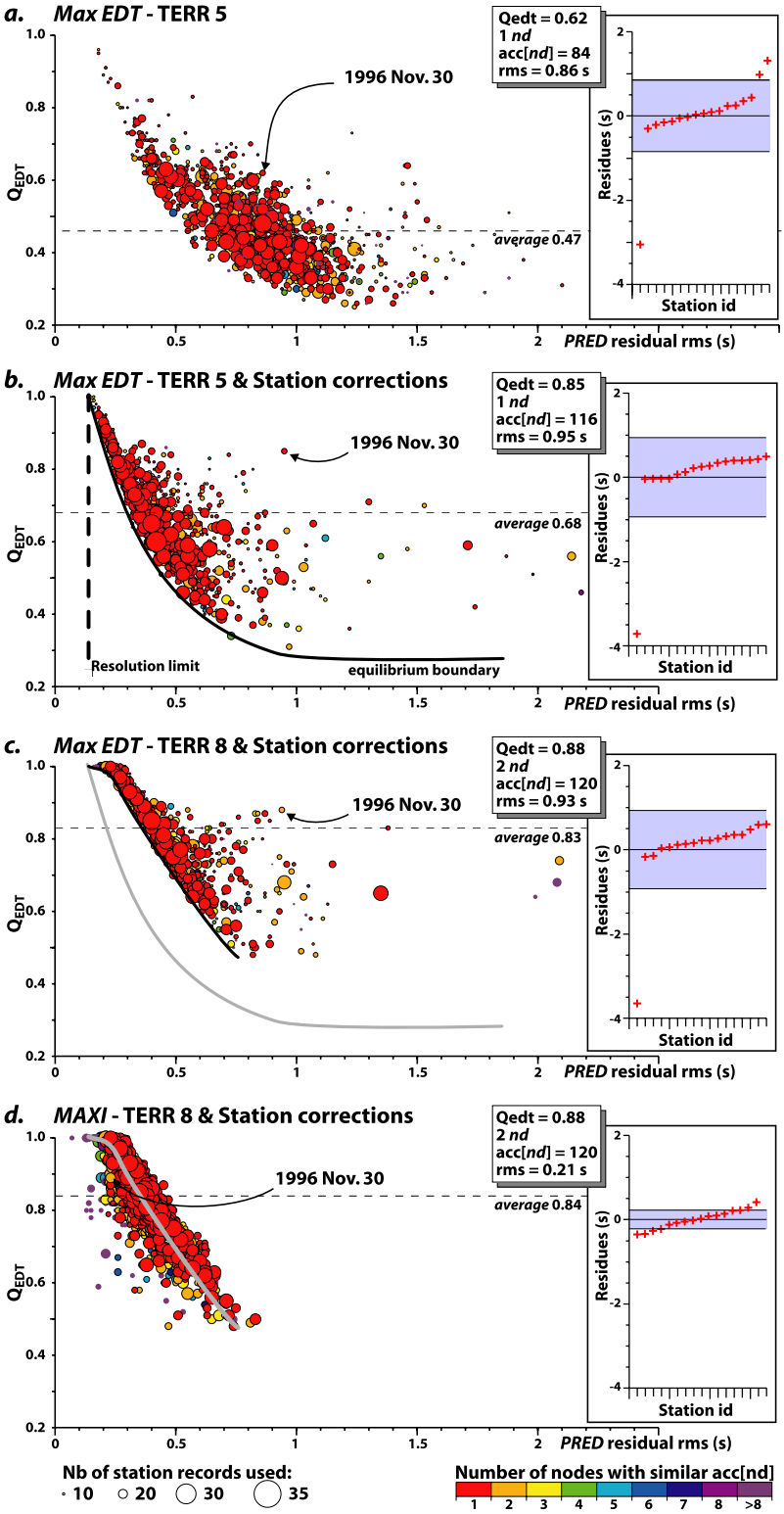

Figure 4. Q_{EDT} versus residual rms (root mean square of the statistical variance) for four distinct relocation procedures (for all 1139 events). (a) Maximum EDT procedure applied with TERR = 0.5 s. (b) Maximum EDT procedure applied with TERR = 0.5 s and station correction. (c) Maximum EDT procedure applied with TERR = 0.8 s and associated station corrections. (d) Maximum intersection procedure applied with TERR = 0.8 s and associated station corrections. Each circle corresponds to one earthquake; its size indicates the number of seismic stations involved; its shade indicates the number of nodes crossed by the same maximum number of EDT surfaces. Note the strong inverse correlation between both Q_{EDT} and rms factors. Details on residual distribution for one anomalous earthquake (1996 November 30) show that incongruent residues strongly affect the rms value but not the Q_{EDT} factor.

Downloaded from https://academic.oup.com/gji/article/158/2/655/771828 by guest on 01 February 2021

the intersection of EDT surfaces, on the other hand, could be more than 30 km in depth. We may therefore ask if residual statistics are a suitable factor for qualifying the accuracy of the relocation results.

Objective detection of outliers

In order to objectively detect outliers, we establish a new quality factor to define the probability of the PRED solution satisfying the whole arrival time data set. We call that quality factor Q_{EDT}. Q_{EDT} is the ratio between the maximum number of EDT surfaces crossing through the PRED node (acc[PRED] in eq. 6) to the total number of EDT surfaces involved in the process (which depends on the number of stations recording the earthquake arrivals, see eq. 4). The Q_{EDT} that characterizes the PRED node is thus defined by

$$Q_{\mathrm{EDT}} = \frac{\mathrm{acc[PRED]}}{C_2^J} \tag{6}$$

Q_{EDT} is unitless and varies from 0 to 1. A value of 0 would mean that no EDT surfaces traverse the PRED node while a value of 1 means that 100 per cent of the existing EDT surfaces intercept the PRED node. Note that, in order to decontaminate the original data set from eventual outliers, the Q_{EDT} factor is always computed at the PRED location with the whole arrival time data set.

In the following, the PRED solutions are obtained for a set of earthquakes occurring offshore of eastern Taiwan ($\sim$1000 events, see later for details about the data), applying the appropriate correction term at each seismic station and with a TERR parameter of 0.5 s (similar to those of Zhou (1994) or Kao *et al.* (2000)). Fig. 4(b) presents the relation between Q_{EDT} and the residual rms associated with the PRED solutions of the studied earthquakes. To first order, the Q_{EDT} and rms factors show a strong inverse correlation with low rms tied to high Q_{EDT} values. The inverse correlation is independent of the number of seismic stations involved during the relocation process and of the number of nodes that are traversed by the same maximum number of EDT surfaces (a case of multiple PRED). We further observe that the Q_{EDT} versus rms distribution tends toward an equilibrium boundary (Fig. 4b) below which no earthquake is found. This quake-free domain strictly indicates that no quakes with low Q_{EDT} can be judged reliable. Thus, the Q_{EDT} quality factor behaves satisfactorily and the Q_{EDT}–rms inverse correlation consequently demonstrates the robustness of the relocation process.

Within the equilibrated domain (i.e. above the equilibrium boundary), most of the seismic events are distributed in a dense cloud that clusters near the equilibrium boundary. The hypocentral location accuracy of the anomalous events (relatively to the earthquake cloud) is at first sight not easy to qualify because, in such cases, the rms and Q_{EDT} factors *seem* inconsistent. Let us take an example of the earthquake which occurred on 1996 November 30 (Fig. 4b). This event ($M_{\mathrm{L}} = 3.7$) was recorded by 17 stations. It presents an incoherent correlation between a good Q_{EDT} value (85 per cent of EDT surfaces cross through the PRED node) and a relatively poor residual rms (0.95 s). Which one of the two factors should prevail to define the quality of the hypocentral determination?

A close view of the distribution of the traveltime residues per station shows that all residues are closely distributed around an average value (about 0.2 s), except for a single residue (at -3.6 s, Fig. 4b) which is associated with an arrival measurement which is obviously flawed. This residual pattern indicates that the hypocentre has been well evaluated by the intersection of EDT surfaces (high Q_{EDT}) and that the outlier residue, probably related to a poor reading, is obviously responsible for the high rms value. Therefore, while the Q_{EDT} factor offers a good definition of the quality of the hypocentral determination, the residual statistics does not properly characterize the accuracy of the location.

To summarize, the Q_{EDT} versus rms diagram shows that the location of PRED nodes is well estimated, even when rms values are large, because the *pre-determination step* automatically and objectively filters the outliers from the original seismic data. In the case of one spurious measurement (i.e. one outlier) at the ith station in a network of J seismic stations, the set of $(J-1)$ EDT surfaces combined with the ith station will be biased while the remaining surfaces ($[J(J-1)/2] - (J-1)$ surfaces) are not corrupted by the wrong measurement and will still intersect the PRED node. The MAXI method thus objectively detects outlier(s) from the original set of data while searching for the PRED node. Prior to the *minimization* process (search for the FINAL solution), it is thus necessary to clean out the data, i.e. to remove the anomalous residue(s) from the original data set (Fig. 3c).

Removing the outlier(s)

Once the PRED location is established (which is accurate to the error uncertainty of TERR), we then compute traveltime residuals. Two statistical techniques are combined to delimit the threshold that defines the outliers: (1) a specific cut-off and (2) an automatic statistical procedure. The cut-off value results from a statistical investigation conducted on the distribution of all residues (all earthquakes, all stations) for the earthquakes relocated *prior* to the outlier decontamination. The specific cut-off is fixed at ± 2.5 the computed rms and we then remove, for each earthquake, all residues that lie outside the range of ± 1.56 s. However, this relatively high cut-off has also been contaminated by a few and very large outliers (>10 s). The use of the second statistical criterion is therefore necessary. The automatic statistical procedure removes all residues that exceed the range of ± 2.5 times the computed rms relative to the residual average (for each earthquake). This procedure consists of accepting that $\sim$97 per cent of the statistical population can be considered as normal compared with the original data set and $\sim$3 per cent should be removed. Note that the automatic procedure will specifically require the cut-off technique when more than one outlier affects the arrival time data set.

In case of multiple PRED solutions, a similar computation is done at each location and the resulting 'cleaned rms' are then compared. The PRED solution that presents the lowest cleaned rms is considered as the closest from the hypocentre. If PRED solutions show equal cleaned rms, the multiple PRED nodes are submitted to the last process: the minimization step.

The minimization step

The location of the PRED solution approximates the hypocentre location because of the use of the tolerance parameter TERR that thickens the EDT surface and the original grid setting. Therefore PRED cannot be considered as the FINAL solution. However, because each EDT (except in the case of outliers) contains the hypocentre location, the PRED solution should depart (at maximum) from the hypocentre location of a distance lower or equal to TERR $\times V_p$. Therefore, it is justified to search for the hypocentre location in the neighbourhood of PRED. Consequently, the last step of the location procedure conducts a forward search for the FINAL solution within

Downloaded from https://academic.oup.com/gji/article/158/2/655/771828 by guest on 01 February 2021

a restricted domain centred on PRED. The FINAL solution is the spatial node that minimizes the rms of the residual variance (eq. 5).

IMPLEMENTATION OF THE MAXI METHOD

One of the advantages of the MSM implementation follows from the reference file that stores the ray tracing results from each seismic station to all nodes in the dense grid covering the modelled region. In the MAXI algorithm, the book-keeping system is strictly identical to the one described by Zhou (1994) who applied the *shortest path method* (Moser 1991; Moser *et al.* 1992) to compute the shortest ray tracing solution. In the following text, we will therefore focus the MAXI implementation on the application to the Taiwanese case and the reader should refer to Zhou (1994) for further details about the book-keeping system. The procedure is nevertheless summarized here below.

Procedure

The MAXI algorithm procedure basically consists of two preparation steps (ST1 and ST2) that are taken just once, and five relocation steps (ST3 to ST6) that are part of the relocation process itself and will be reiterated for each seismic event, as each is independently relocated (Fig. 3).

ST1 creates the reference ray tracing file for all available seismic stations in the dense grid of blocks and nodes that characterize the 3-D heterogeneous velocity model of the Earth's structures. First, rays are computed from each node in the entire velocity model to each seismic station, using the *shortest path method* (Moser 1991; Moser *et al.* 1992). Second, all computed traveltimes are stored in a single reference file. Consequently, a unique computation of all traveltimes is sufficient and each earthquake location procedure will call for a simple search through the traveltime table. ST2 inputs in individual files all *P* arrival times—generated by individual earthquakes—recorded at each station. ST3 sets the TERR parameter, inserts the *P* arrivals in the obs[*J*] array, where *J* is the total number of records for an earthquake, and inputs the seismic station correction term (when available). ST3 also initializes an acceptance vector acc[*M*] to value 0, where *M* is the total number of ray tracing nodes. ST4 computes the arrival time difference observed at any pair of stations and consults the reference file to update the acceptance vector at each node in the model. Consistently, each time a node satisfies the time difference $\pm$ the TERR value, i.e. each time a node is traversed by a thickened EDT surface, a value of 1 is added to the acc vector associated with that node. One condition restricts the shape of the EDT surface: the updated nodes must be located outside the water column or soft sediments (the velocity related to the node must be at least greater than 3 km s^{-1}). ST5 identifies the preliminary determination (PRED), which is the node traversed by the maximum number of EDT surfaces. In other words, ST5 selects, among all nodes, the one(s) with the larger acc[*M*] value. The residual average and variance are then computed for the PRED node(s) and spurious station records (if residual outliers are detected) are removed from the obs[*J*] array. In the case of multiple nodes with equal maximum value of acc[*M*], the node presenting the smallest residual RMS will undergo ST6. ST6 conducts a forward search around PRED seeking the FINAL solution that minimizes both residual statistics presented in eqs (5) and (7). The size of the searched volume is restricted to $\pm$10 km in the horizontal directions and $\pm$6 km in the vertical directions. A computation of residual statistics is executed at every kilometre, in the *x*, *y* and *z* directions.

Three-dimensional velocity model

Due to the inhomogeneous station coverage of the local seismic networks there is no detailed tomographic study offshore of eastern Taiwan. Nevertheless, since 1991 several oceanographic surveys have collected bathymetric and geophysical data in the region providing new constraints on the 3-D crustal structures. We compiled (Fig. 5) seismic reflection and refraction profiles based on the work of Cheng *et al.* (1996), Dominguez *et al.* (1998), Font (1996, 2001), Font *et al.* (2001), Hagen *et al.* (1988), Hetland & Wu (1998, 2001), Hirata *et al.* (1991), Lallemand *et al.* (1997a, 1999), Liu (unpublished data), McIntosh & Nakamura (1998, 1999), Schnurle *et al.* (1998a,b), Wang & Chiang (1998), Wang & Pan (2001), Yang (1999), Yang & Wang (1998), the earth model iasp91 (Kennett & Engdahl 1991) and global seismicity (Engdahl *et al.* 1998).

Accordingly, we have integrated all geophysical data in order to built a 3-D comprehensive velocity model in the offshore domain. To construct the offshore velocity model, we define the envelopes of the structural bodies existing in the offshore domain. The main structural bodies investigated concern the sedimentary layer, the crustal basement and part of the upper mantle. The consistency among different data sets used in the compilation is carefully checked at the overlapping zones or the intersections between any two models, and the shape of the envelopes is established in the spatial volume. The reader is invited to refer to Font *et al.* (2003) for details about the interpolation between different data and to original publications to obtain specific information and details about the acquisition, processing and resolution limits of each data set.

The offshore model is then combined with an onland tomographic model (Rau & Wu 1995) to create the first comprehensive 3-D V_p model for the region (Font 2001; Font *et al.* 2003). The model extends from eastern Taiwan to the neighbouring Japanese islands. It covers the area from 121.0°E–124.4°E and 22.0°N–25.3°N, down to 120 km. The velocity model includes the water layer, sedimentary structures (e.g. Ryukyu forearc basins and accretionary prism), the thin oceanic crust of the Huatung and West Philippine basins, the thickened crust of the Luzon Arc, the subducted Philippine Sea slab, the curved Ryukyu margin and the thinned South Okinawa backarc continental crust (Fig. 5).

For application to hypocentre determination, the velocity model is organized into a blocky schema, following the approach presented by Zhou (1994). Horizontally, the studied area covers 350 $\times$ 370 km^2, with *x* and *y* axes following east–west and north–south directions respectively. The southwestern corner is assigned to be the point of origin, at 120.95°E–22.00°N. The heterogeneous velocity structures are characterized by a set of non-overlapping, equal volume and constant-V_p velocity blocks. Each block dimension is 10 $\times$ 10 $\times$ 3 km in the *x*, *y* and *z* directions respectively. Thus, the entire velocity model consists of 35 $\times$ 37 $\times$ 40 = 51 800 blocks.

In accordance with the shortest ray path method in a 3-D model (Moser *et al.* 1992), ray tracing nodes are placed only on facets, edges and vertices of blocks and each of them has a constant slowness ($1/V_p$). Because blocks are of constant velocity, i.e. there is a straight ray path within each block, there is no need for nodes inside the blocks. The interval between two adjacent nodes is 2 km along the horizontal directions and 1 km vertically. Each block consists of 88 nodes and 2 303 456 nodes constitute the whole velocity model. The size of the reference file that stores the pre-computed ray

Downloaded from https://academic.oup.com/gji/article/158/2/655/771828 by guest on 01 February 2021

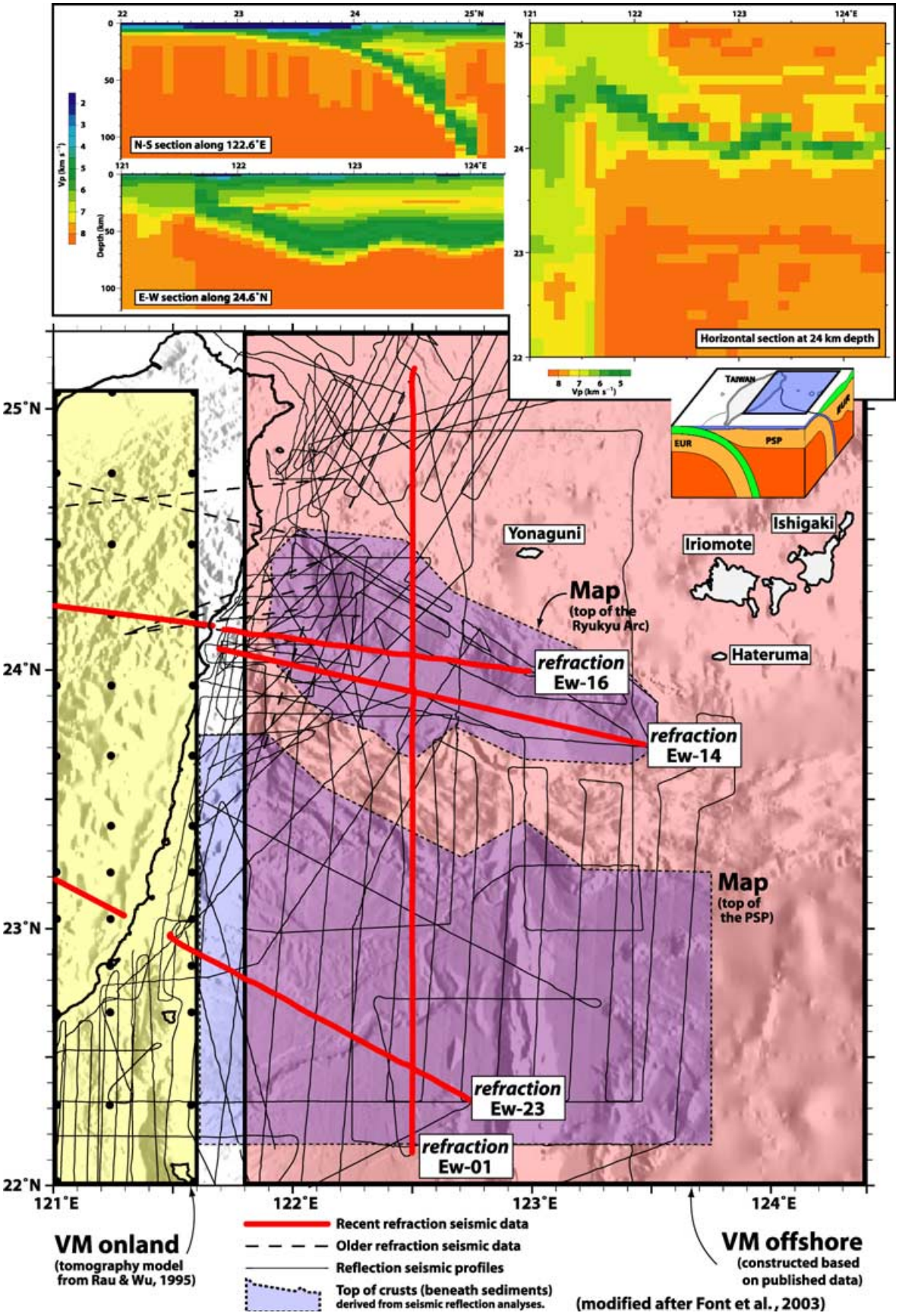

Figure 5. Bottom: coverage of the different data sources used to construct the 3-D velocity model offshore of eastern Taiwan. Top: examples of vertical and horizontal cross-sections within the 3-D velocity model.

Downloaded from https://academic.oup.com/gji/article/158/2/655/771828 by guest on 01 February 2021

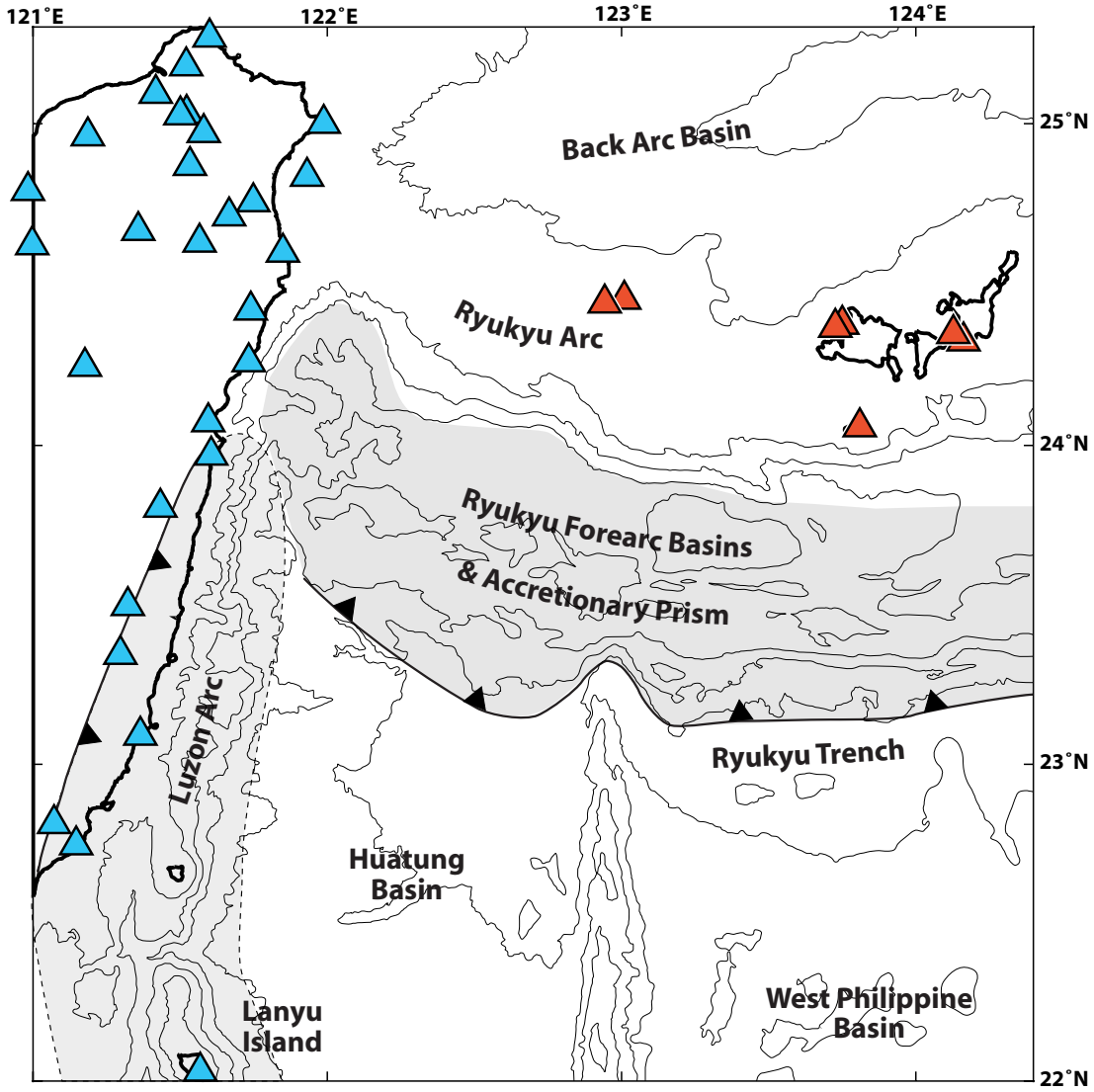

Figure 6. Distribution of the seismic stations used in this study (grey triangles, Taiwanese Central Weather Bureau (CWB) seismic stations; white triangle, Japanese Meteorological Agency stations). Note that only four seismic stations coexist at a time on the Japanese islands (three of them have been slightly moved during the period of time under study).

tracings exceeds 750 Mb, which is the main limiting factor for the size of our velocity model, the dimension of blocks and node intervals.

Seismic data

We improve the offshore earthquake azimuthal coverage by combining the data from the two independent networks that surround the study area: the CWB from Taiwan and the JMA seismic networks. We select all seismic stations distributed in the velocity model with an elevation lower than 2 km and that continuously recorded from 1992 to 1997. Our set of seismic stations is composed of 29 Taiwanese stations distributed along the eastern coast between northern Taiwan and Lanyu Island, and four Japanese stations located on the closest Japanese islands (Fig. 6).

The discrepancies in horizontal location between Taiwanese and Japanese hypocentral determinations are extremely large (60 and 25 km, on average, for events of M_L smaller and larger than 4, respectively). Consequently, the search for events common to both catalogues is relative to the time of origin of each earthquake (and not to the location) and refers to earthquakes nucleating within the studied domain (after the CWB source). Note, however, that the Taiwanese network has a limited resolution in recording earthquakes occurring east of 123°E and that therefore an empty catalogue is expected between 123 and 124°E.

All the selected earthquakes have been recorded by at least seven of the Taiwanese stations (with a very good to good quality estimate) and at least three of the four Japanese stations. Between 1992 and 1997, we obtain 1139 seismic events common to both seismic networks, with a minimum of 10 *P* arrival records by earthquake, for a total of 28 514 *P* arrival times.

FROM THE MSM TO THE MAXI METHOD

The objectives of this investigation are two-fold: first we aim to improve the earthquake location offshore of eastern Taiwan and second to examine the robustness of the MAXI method, both objectives being closely related.

Downloaded from https://academic.oup.com/gji/article/158/2/655/771828 by guest on 01 February 2021

When testing several codes that would result in several sets of seismicity data for the same area, it is important to realize that assessing which one of the location procedures is optimum is not easy, especially in 3-D, because quantitative measures of earthquake clustering (such as the entropy method suggested by Nicholson *et al.* 2000) are still very difficult to evaluate. Therefore, we assess the first goal by comparing the relocated data with the original Taiwanese catalogue in terms of residual statistics and earthquake distribution. To address our second goal, because Taiwanese hypocentral determinations are established in a standard 1-D velocity model with a different data set (with seismic stations only distributed on the whole island of Taiwan), we compare MAXI with the MSM through improvement of hypocentral location.

Using the same 3-D velocity model, the main aspects of the MAXI method are investigated by a series of test procedures that progressively modify the original MSM. The results of each test procedure lead to new modifications on the algorithm that becomes the next location procedure. This section aims to synthesize those procedures and associated results. Consequently, we will show here different sets of earthquake determinations resulting from:

(1) The original MSM.
(2) A first intermediate step: the maximum EDT applied with a TERR parameter of 0.5 s.
(3) A second intermediate step: the maximum EDT applied with a TERR parameter of 0.5 s and the appropriate station corrections.
(4) A third intermediate step: the maximum EDT applied with a TERR parameter of 0.8 s and the associated station terms.
(5) The MAXI method applied with a TERR parameter of 0.8 s and the associated station terms.

Note that MSM and the MAXI algorithm read, as part of their input information, the location parameters from the CWB hypocentral determination. The algorithms subsequently compute the CWB residual rms, within the 3-D velocity model, using the original CWB location and the same set of seismic arrivals as used in the relocation process. Consequently, to compare residual statistics between CWB and the relocated earthquake we use the value computed by the algorithm (that differs from the ones given in the CWB catalogue).

Master station determinations

Basically, the original MSM differs from the MAXI method in three main points:

(1) During the updating procedure (ST4, Fig. 3), only $J - 1$ EDT surfaces (in a network of J stations) are used to search for the PRED node, which correspond to the number of station pairs combined with the 'reference station' alone (the master station St_0 that recorded the earliest arrival time).
(2) Outliers are not removed.
(3) During the FINAL procedure (ST6, Fig. 3), the statistical minimization is conducted in the whole velocity model space, starting from the PRED node.

The MSM is applied with a TERR parameter of 0.5 s. Compared with CWB, the quality of the MSM determinations is already improved considerably as shown by the average residual rms reduction from 1.2 to 0.8 s and by the spatial earthquake distribution that is less scattered (Fig. 7). This improvement can be attributed to a combination of (1) the 3-D velocity model (versus 1-D for CWB), (2) the increase in the azimuthal coverage (combined networks) and (3) the MSM procedure. Indeed, even though the population of EDT surfaces involved in the relocation is much smaller in the MSM than in the MAXI method, the process of EDT intersection should also, theoretically, discard spurious measurements from the original data set. Two observations, however, lead us to modify the MSM.

First, among the MSM-relocated earthquakes, 267 events are located in the water and 60 of them have the same reference station, St_0. In order to test the dependence with St_0, we have then conducted a series of trials using synthetic data by perturbing the St_0 arrival time. The resulting solutions show that a shift in the St_0 arrival time (or the deletion of this record) produces significant variations in the PRED location, while a shift (or the deletion) brought to another seismic station does not modify the PRED solution. This observation illustrates that even though the EDT surfaces are independent of each other they are indeed strongly dependent on the reference station arrival time. In other words, if an outlier affects the station of reference, St_0, then the whole set of EDT surfaces is flawed and the hypocentre determination is shifted in space.

To avoid the St_0 dependence, we increase to the maximum the number of EDT surfaces by combining all possible station pairs. This choice is obviously time-consuming (compared with MSM), but the hypocentre has every chance to be better located because the set of flawed EDT surfaces ($J - 1$ surfaces) associated with one spurious arrival measurement will be counterbalanced by the increased number of unbiased surfaces $[J(J - 1)/2] - (J - 1)$.

Second, the study shows that 58 events have a depth difference greater than 10 km between PRED and the FINAL solutions. On average, the depth difference reaches 18 km, with a maximum of 56 km. The MSM minimization process obviously generates erroneous FINAL determinations that greatly depart from the PRED location. We relate this to two main causes: either spurious measurements often intrude into the original data and affect the minimization process or the FINAL search often falls into local minima. In any case, to avoid a great departure from the PRED solution, that statistically defines the node with a greater probability of representing the hypocentre, we modify the algorithm to confine the minimization process to a small volume centred on PRED (Fig. 3d).

Maximum EDT determination

The 'maximum EDT' process increases to the maximum the number of EDT surfaces involved in the relocation process (eq. 4), restricts the minimization search to a small volume around PRED and does not allow the determination to be located in the water or soft sediments.

Between the *maximum EDT* and CWB determinations, the average rms is reduced by 40 per cent (it decreases from 1.2 to 0.77 s, Fig. 7). The drop in rms between the MSM and the *maximum EDT* determinations seems, when one examines FINAL relocations, to be less significant than expected (from 0.8 to 0.77 s). This is due to the fact that the MSM minimizes the FINAL solution over the whole space of the velocity model, which can, as explained above, often be inappropriate but will still result in low (to very low) rms values. The quality consistency of the results should therefore be checked in the PRED determination. The residual histograms for PRED solutions (of all relocated quakes) show an average of 0.89 s and 0.87 s for the MSM and the *maximum EDT* process respectively. Again, the rms diminution is less significant than expected and the improvement in earthquake location is mainly assessed from the clustering observed in the earthquake distribution (Fig. 7).

At this stage, we can establish the Q_{EDT} parameter because the number of EDT surfaces is increased to its maximum. The first

Downloaded from https://academic.oup.com/gji/article/158/2/655/771828 by guest on 01 February 2021

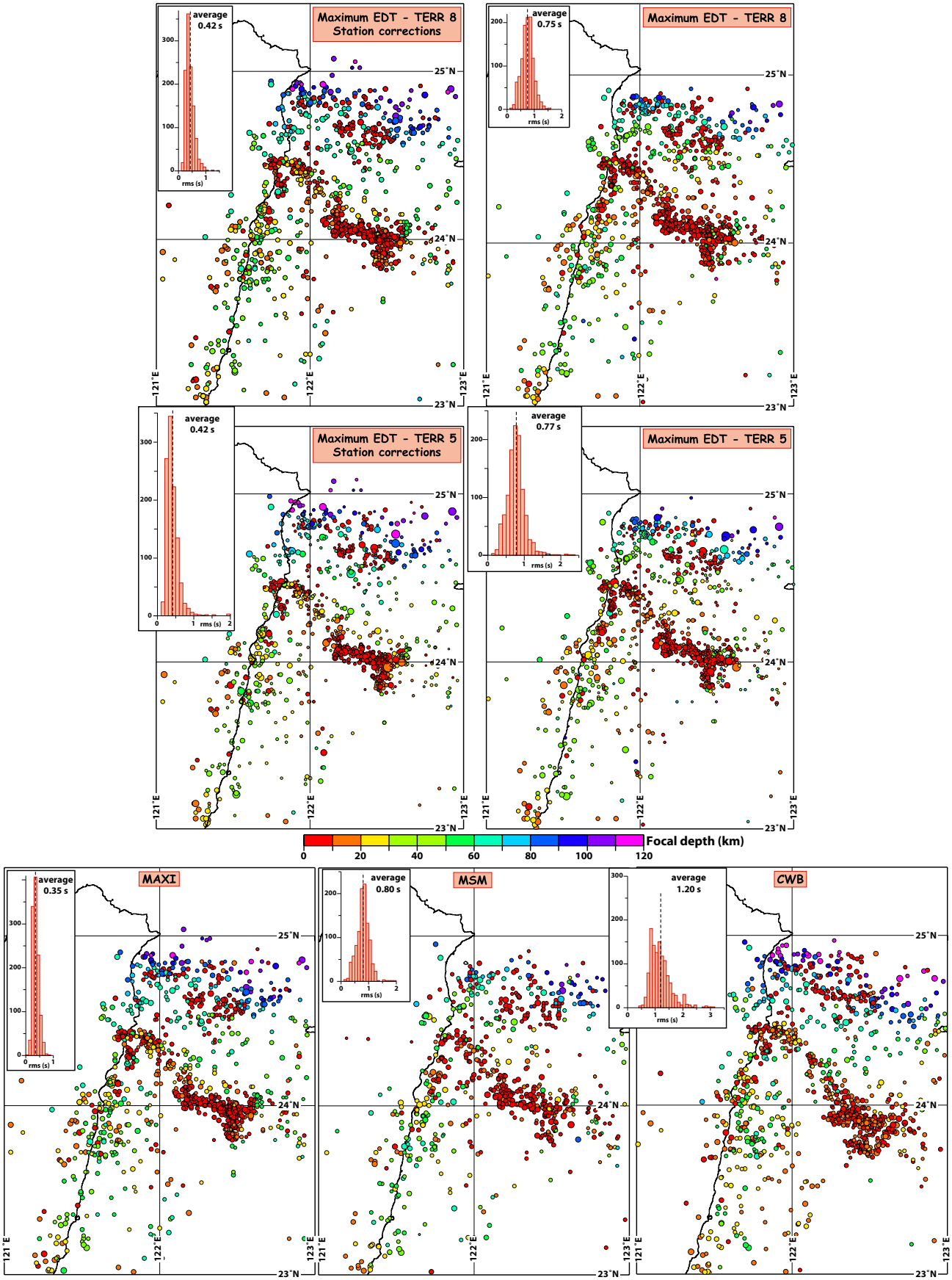

Figure 7. Hypocentral determinations and associated residual histogram for the distinct procedure steps discussed in the text.

Downloaded from https://academic.oup.com/gji/article/158/2/655/771828 by guest on 01 February 2021

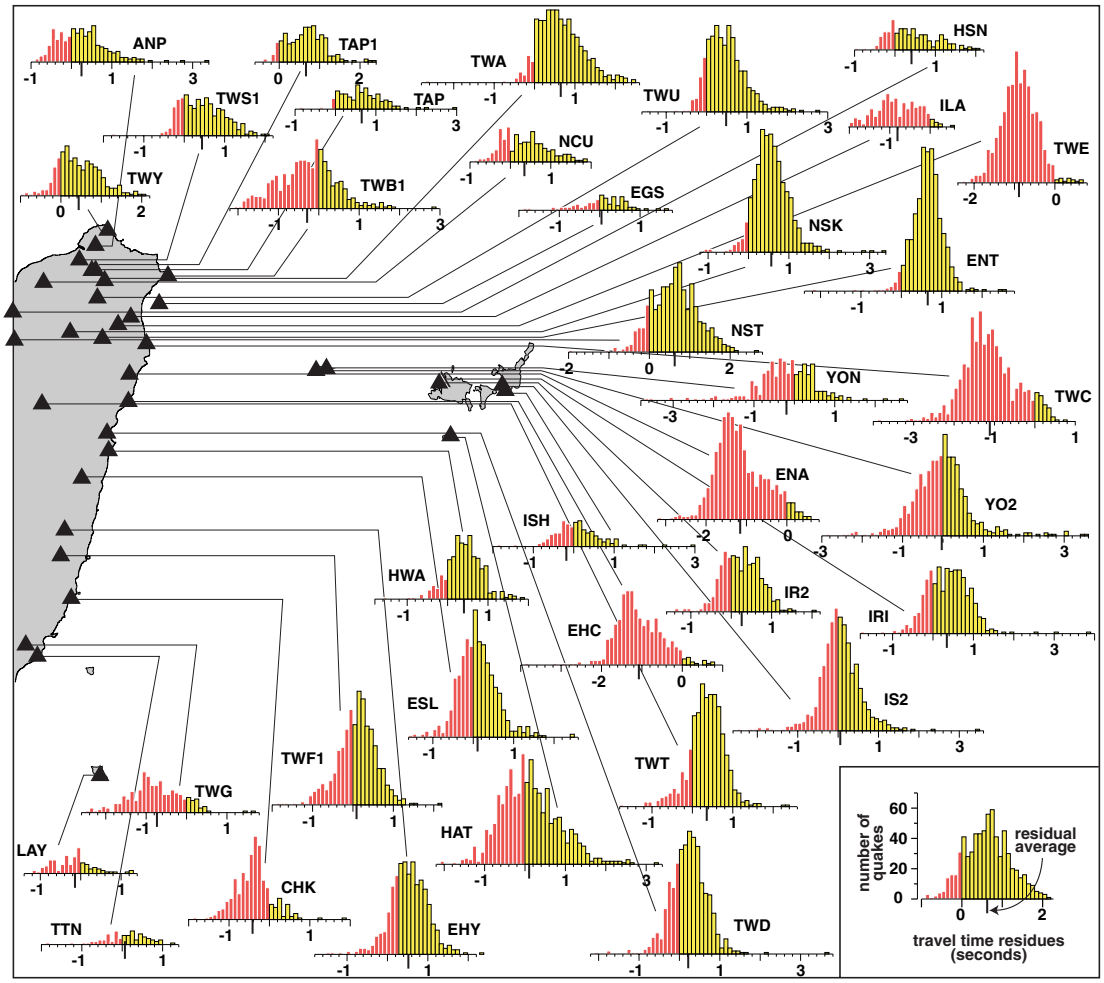

Figure 8. Histograms of traveltime residues per seismic station (for the whole hypocentre set relocated in this study). Positive residues are black while negative residues are white. The residual average (on the abscissa axis of the histograms) is used as the station correction term.

purpose of this parameter is to introduce an alternative way to assess the quality of the relocation that is totally independent of traveltime residues. The Q_{EDT} versus rms diagram shows a good inverse correlation, but the averaged Q_{EDT} factor for the set of earthquakes is low (0.47, Fig. 4a). In contrast with the residual rms, we have seen that the Q_{EDT} factor is totally independent of traveltime residues and estimated earthquake origin time. Q_{EDT} does in fact depend on parameters intrinsic to every hypocentral location method such as velocity model inaccuracies, approximations done on ray path computations, velocity model gridding limitations and *P* arrival measurements. The Q_{EDT} factor therefore provides a statistical index on the coherence of measured *P* arrivals relative to the unknown parameters (x, y, z), with respect to the velocity model. When only 47 per cent of the EDT surfaces traverse the PRED solution, it means that the remaining 53 per cent disagree with this hypocentral position. To a first approximation, if the improvement of the relocations reflects the use of the 3-D velocity model, the relatively low Q_{EDT} average value indicates that there is a lack of coherence between the seismic data and the ray tracing computed in the velocity model. Because the 3-D velocity model has been established on the basis of multiple geophysical data sources (Font 2001; Font *et al.* 2003), it is therefore necessary to check in more detail the behaviour of traveltime residues with respect to the seismic data.

Residual histograms per station (for all earthquakes) show that most of the residue distributions are unimodal, i.e. approximately symmetric to their averaged value (Fig. 8). On average, for each station the standard deviation implies that about 95 per cent of the residues spread within the ±1.3 s range centred on the average (that differs from zero). Generally, residues related to random noise spread (widely or not) around zero. Residues related to velocity anomalies that accumulate *along* the ray path concentrate along one single 'pick' (unimodal distribution) only if all rays follow a similar path (and therefore generate similar residues). In the case of several clusters (i.e. different ray paths), the unimodal spreading of residues, with an average not centred on zero, most certainly accounts for a combination of random noise and of a significant velocity anomaly located immediately beneath the seismic station. Indeed, residual averages are rarely null in this study but are more often offset toward positive (Fig. 8, ENT station) or negative values (TWE station). This result leads to algorithm modifications that consist of including station terms to account for the bias of local anomalies existing in the velocity model.

Maximum EDT and station corrections

The *maximum EDT and station correction* procedure is similar to the *maximum EDT* one, except that each seismic station is corrected by an offset term. In absolute terms, about 5 per cent of the residues exclude the ±4 s interval and are distributed randomly with respect

Downloaded from https://academic.oup.com/gji/article/158/2/655/771828 by guest on 01 February 2021

to the station (three eccentric values per station, at maximum). We related those flawed residues to isolated large measurement errors. Consequently, the offset term at each station equals the residual average, after removal of the eccentric values.

The consideration of a single offset term leads to significant improvements in hypocentral locations based on residual statistical observations. The average residual rms (0.42 s) decreases by 66 per cent and by 45 per cent compared with the CWB and the maximum EDT average, respectively (Fig. 7). This improvement is also confirmed by the clustering of seismic events along well-known tectonic features (such as, for example, the Hoping Canyon or the Hoping Basement High, Font 2001, Fig. 7). From the Q_{EDT} statistical analyses, the contribution of the station correction increases the number of EDT surfaces passing through the PRED node to 68 per cent, on average. Therefore, the station corrections had improved the statistical coherence between seismic observations and ray tracings, which illustrates the reliability of the correction terms used to adapt the velocity model and seismic data. The Q_{EDT} versus rms diagram attests to this improvement by gathering the earthquake cloud toward the low-rms/high-Q_{EDT} domain (Fig. 4b). The combined Q_{edt} versus rms factors are therefore good indicators of the quality of the relocation. Let us take the case of the 1996 November 30 earthquake, the original data set of which contains one spurious measurement. The station correction effect is evidenced by comparing the residual distribution with the previous location procedure (i.e. without station correction). All residues are now closely distributed around 0.2 s (augmentation of the coherence), except the one associated with the flawed arrival measurement, that increases to ∼0.7 s. Thus, station correction terms better account for traveltimes and emphasize even more outliers.

Nevertheless, the Q_{EDT} factor is affected by the TERR parameter, which controls the thickness of the EDT surface. An appropriate evaluation of TERR should tolerate small picking errors (random noise) within the EDT surface and exclude spurious measurements so that the surface intersections can properly filter incongruent data. Indeed, the variation of the TERR parameter influences the size of the volume defined by the intersection of EDT surfaces and consequently affects the threshold value under which no outliers can be detected. To estimate what TERR parameter best suits our data, we perform a series of hypocentral determination processes applied to a subset of seismic data (∼320 earthquakes located between 122–122.7°E and 23.7–24.2°N).

Each process is executed with a TERR value varying from 0.1 to 1.2 s, with an increment of 0.1 s, and an extreme test is performed at TERR = 2.0 s (note that no station correction is applied, see Fig. 9). As expected, the average Q_{EDT} increases steadily from TERR = 0.1 s to TERR = 2.0 s while the average residual rms decreases. When EDT surfaces are too thick (TERR = 2.0 s, Fig. 9), the search for PRED is not optimized because the thick EDT intersections define a very broad volume where several nodes are traversed by the same maximum number of surfaces. In this situation, the selected PRED node corresponds to the one presenting the smallest rms and the ultimate solution will therefore approximate the search by residual minimization. Furthermore, when EDT surfaces are too wide, they tolerate all error types equally (including spurious measurements) and in such a case outlier cleaning becomes impossible (note that on Fig. 9, for TERR = 2.0 s, only two events fall outside the dense earthquake cloud). On the contrary, when EDT surfaces are too thin (TERR = 0.1 s, Fig. 9), absolutely no error types are tolerated (including the random noise associated with *P* measurements). Consequently, during the pre-determination step a small number of EDT surfaces will intersect at a large number of spatial points (low Q_{EDT}) and the random rms distribution (relative to the Q_{EDT} variations) confirms that this alternative is not suitable. Note that in this case, the earthquake cloud is so dispersed that no outliers can be identified. Only an adequate evaluation of TERR can ascertain that the node intersected by the maximum number of EDT surfaces is indeed very close to the hypocentre. The curve described by the average of residual RMS for each trial (Fig. 9) includes two asymptotic portions and thus presents two optimal points, at 0.5 and 0.8 s. The residual distribution for the seismic events that exclude the earthquake cloud on Q_{EDT} versus rms diagrams (presumably containing outliers) favours the value of TERR = 0.8 s. The variation of the number of nodes traversed by the same maximum number of EDT surfaces (acc[*nd*]) when TERR augments versus the maximum number of EDT surfaces intersecting PRED corroborates this choice. A TERR value of 0.8 s is certainly most appropriate to optimize our data set (Fig. 9). This information triggers the next relocation, which does not result from a modification of the algorithm but from the change of TERR parameter.

Maximum EDT and TERR 0.8 s and station corrections

The *maximum EDT* procedure applied with a TERR parameter of 0.8 s proceeds in two separated steps: (1) without station corrections and (2) with station corrections. In the present investigation, the station terms computed with TERR = 0.8 s are similar to the ones associated with TERR = 0.5 s. The drop of residual rms (to an average of 0.75 and 0.42 s, without and with station corrections respectively, Fig. 7), the increase of the Q_{EDT} parameter (0.62 and 0.83, with and without station corrections respectively), and the clustering of earthquakes relocated with a TERR value of 0.8 s confirm the adequacy of our choice.

On the Q_{EDT} versus rms diagram, the location and shape of the earthquake cloud have evolved from earthquakes relocated with TERR = 0.5 s to TERR = 0.8 s (with the maximum EDT procedure and station corrections, Figs 4b and c). The earthquake cloud not only migrates toward high-Q_{EDT} and a low-rms domain, but is also much gathered onto the equilibrium boundary. In addition, eccentric earthquakes still prevail (high-rms domain), which signifies that residual outliers are still excluded from the EDT intersection process. As an example of the exclusion of outliers during the PRED determination, a close view of the residue distribution for the 1996 November 30 earthquake indicates that the incongruent residue is still detected at −3.6 s (Fig. 4c).

At this stage, the algorithm is able to detect outliers from the residual set, but they are not removed from the minimization step. Even though PRED determinations already appear quite satisfactory, the minimization procedure around PRED is still compulsory for two main reasons: (1) the thickness of EDT surfaces limits precise location and (2) the gridding configuration is relatively large, with spatial nodes disposed only on facets, edges and vertices of the empty blocks. The forward search for the node presenting the smaller residual statistics within the blocks is thus adequate for refining the location of the determination.

For the 371 earthquakes containing an outlier in the original data set (which is inferred from MAXI results), the distribution of the distances between the PRED and FINAL nodes indicates that the minimization process results in a FINAL node that departs, on average, by 1.6 km (σ = 1.9 km), 1.7 km (σ = 1.9 km) and 2.3 km (σ = 2.0 km) from PRED along *x*, *y* and *z* respectively; Fig. 10a). This shows that the minimization process is almost stopped by the boundaries of the search volume (fixed at ±10, 10 and 6 km from the

Downloaded from https://academic.oup.com/gji/article/158/2/655/771828 by guest on 01 February 2021

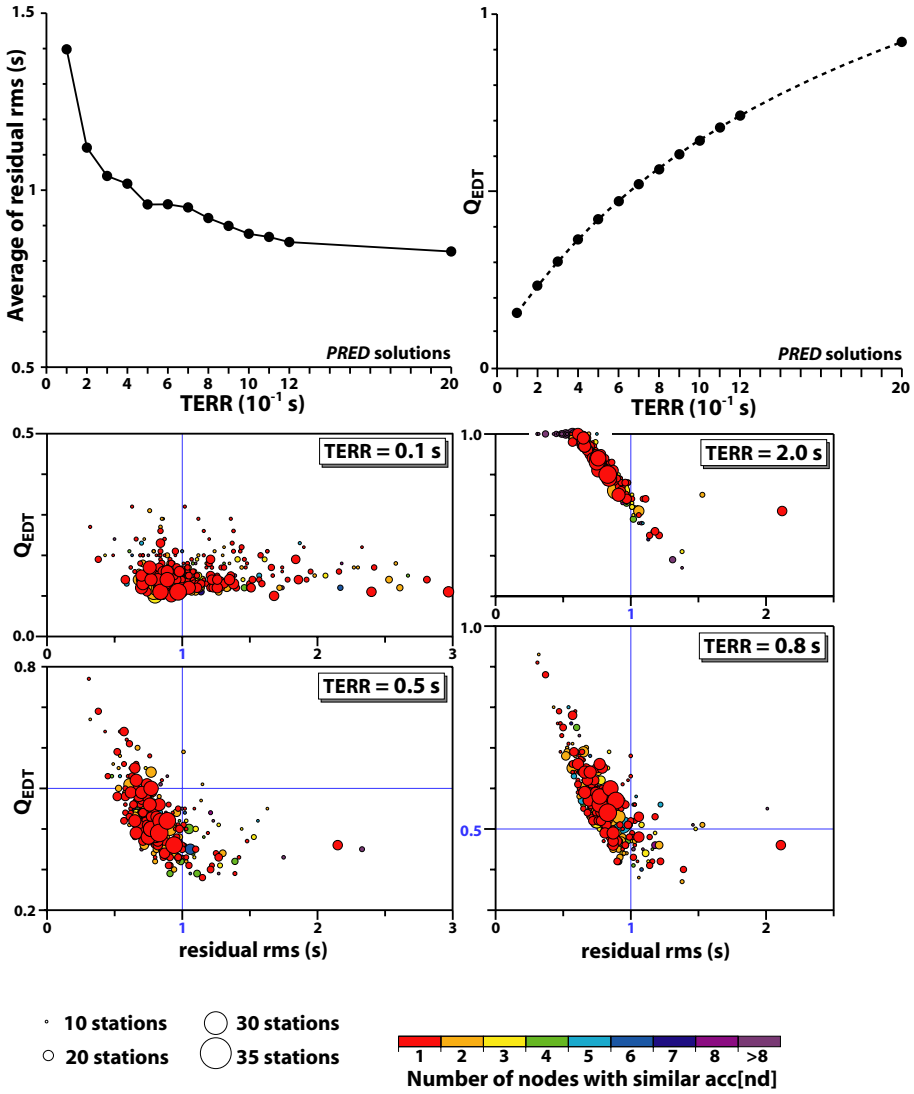

Figure 9. Example of TERR parameter evaluation from a series of hypocentral determinations applied to the same set of ∼320 earthquakes, with a TERR value varying from 0.1 to 1.2 s (increment of 0.1 s) and an extreme test performed with TERR = 2.0 s. The combined observation on the variation of average rms, Q_{EDT}–rms diagrams and the number of PRED solutions determined at each process indicates that a TERR value of 0.8 s should optimize the MAXI algorithm with our set of data.

PRED node position, along the *x*, *y* and *z* axis, respectively) rather than by the finding of the solution. Consequently, it is necessary to first remove the detected outliers from the data set before discussing the minimization process. This ultimate modification leads to the MAXI algorithm.

MAXI—DISCUSSION

Following the above development, MAXI is performed using a TERR parameter of 0.8 s and applying station correction. The drastic decrease in rms compared with CWB (from 1.2 to 0.35 s, on average; Fig. 7) as well as to MSM (from 0.8 s to 0.35 s) shows the achievement of our two main objectives: improvement of the earthquake location in an area presenting a heterogeneous azimuthal coverage as well as an intricate velocity structure, and examination of the robustness of the MAXI method. The increase in average Q_{EDT} (0.84, associated with a standard deviation $\sigma = 0.12$) and the Q_{EDT} versus rms diagram illustrates this improvement. The earthquake cloud again migrates toward the high-Q_{EDT} and low-rms domain (Fig. 4d). Because selection of the PRED node is performed after removing outliers, the earthquake cloud distribution is much more concentrated, and now the anomalous events exclude the cloud toward the '*high-quality*' domain. This rms decrease indicates that we have succeeded in removing the outliers. For example, the algorithm detected and removed one outlier in the 1996 November 30 earthquake. For that event, the outlier deletion produces a location difference of 5.3, 5.9 and 6 km in the *x*, *y* and *z* directions respectively, a residual rms decrease (from 0.93 s to 0.21 s) and an unchanged Q_{EDT} value (0.88).

In this investigation, the outlier selection is performed by (1) cutting off the residues that exceed the ±1.56 s interval and (2) removing those that exceed the ±2.5 rms range. Among the 1139 events in our data set, 371 earthquakes contained one or several eccentric residue(s). In total, 417 eccentric residues have been removed prior the minimization procedure: the cut-off threshold

Downloaded from https://academic.oup.com/gji/article/158/2/655/771828 by guest on 01 February 2021

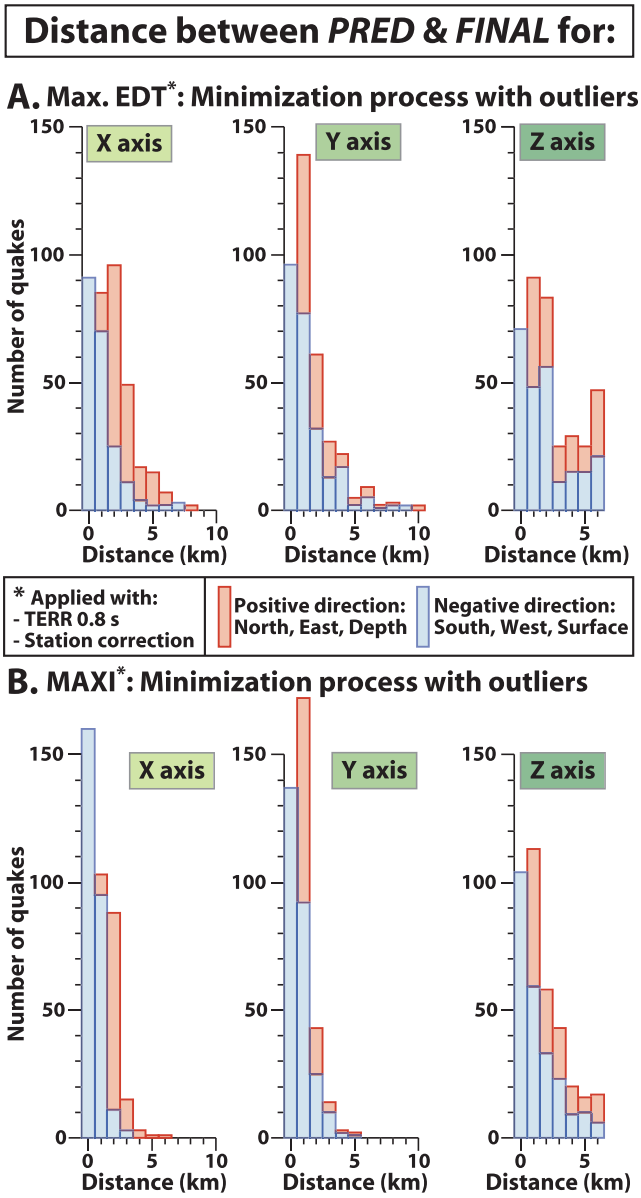

Figure 10. Histograms of the distance from PRED to FINAL along the *x*, *y* and *z* axes for the 371 earthquakes that contain (at least) one outlier: (a) *maximum EDT* procedure; (b) MAXI procedure.

detected 215 residues (average of absolute residues = 2.93 s, standard deviation $\sigma = 7 \times 10^{-3}$ s), and the automatic statistical procedure selected 202 eccentric residues (average of absolutes = 0.83 s, $\sigma = 3 \times 10^{-3}$ s). In terms of distance variation (compared to *maximum EDT* hypocentral determination, Fig. 11c), the removal of the outliers produces a difference in the three spatial directions for 187 earthquakes (average of 3.3 km). Along the *x*, *y* or *z* direction, the average distances reach 2.4 km ($\sigma = 2.6$ km), 2.6 km ($\sigma = 2.9$ km) and 3.9 km ($\sigma = 5.2$ km) for 303, 278 and 268 events respectively. Among the 371 earthquakes containing at least one outlier, only 11 events keep their position unchanged.

The Q_{EDT} versus rms diagram (Fig. 11a) compares the *maximum EDT*-relocated earthquakes with the MAXI-relocated earthquakes that (1) include at least one outlier and (2) result in a different FINAL location. As expected, the earthquakes far outside the cloud in the maximum EDT procedure (see also Fig. 4c) are now shifted in the low-rms domain (Fig. 11a). Some of them even reach a surprisingly low rms (compared with the cloud average), but nothing indicates a bias in the relocation process. Note that for earthquakes including at least one spurious measurement and resulting in the exact same FINAL hypocentral solution (3 per cent of the contaminated events), the rms variation is quite small (Fig. 11b). In terms of seismicity distribution, the impact of outlier deletion on the hypocentral location is (1) not systematic (i.e. in all space directions) and (2) tends to gather the seismic clusters, which attests to the reliability of the MAXI process.

The outlier distribution per seismic station is not homogeneous (Table 1), as confirmed by the large standard deviation ($\sigma = 18.6$) associated with the average number of outliers per station (11.5). In particular, the Japanese seismic station (HAT) has recorded 107 arrivals that have been considered as outliers. At this station the residual outliers are distributed between −4 and +5 s, with a residual average of 0.78 s ($\sigma = 1.89$ s) and an absolute residual average of 1.68 s. Approximately 50 per cent of the eccentric residues are detected by the specific cut-off and 50 per cent by the automatic statistical procedure (Fig. 12). The average Q_{EDT} of those 107 events (0.78 s, $\sigma = 0.10$ s) is slightly lower than average Q_{EDT} of the whole data set (0.84 s, $\sigma = 0.12$ s).

There could be two main reasons for such a concentration of outliers at a single seismic station (namely HAT): (1) arrival picking inconsistencies and (2) the presence of a velocity anomaly in the source–station ray path. Due to the lack of information on the Japanese catalogue, the first reason is difficult to investigate with precision. Such a large picking error might be attributed, for example, to clock drifts. The second reason is examined through the spatial distribution of the seismic events concerned (Fig. 12a). If those earthquakes are concentrated in a unique small volume, we could consequently approximate that the ray paths are similar and deduce that a local velocity anomaly triggers a systematic travel time perturbation from the confined space volume to the specific station. Because the cleaning procedure 'only' detects at HAT ∼110 outlier earthquakes on ∼770 relocated events recorded at HAT, the velocity anomaly cannot be located immediately beneath the seismic station (i.e. be traversed by all ray paths) but should rather be distributed on the specific source–receiver travel paths. In the present case, the outlier earthquake spatial distribution is relatively well concentrated in two clusters (Fig. 12). The rays from the earthquakes to HAT are parallel to the subducting slab; the rays could cross many small inaccuracies in the slab model that may accumulate in many large time errors. However, many other uncontaminated events are located in the same two clusters and they do not produce outliers at HAT (Fig. 12b). Therefore, it is not likely that velocity anomalies generate systematic errors at the HAT station. To explain the concentration of outliers at HAT we tend to favour the first reason, i.e. arrival picking inconsistencies. Note, however, that in a general fashion the detailed analyses of outlier earthquakes per station might be an interesting way of judging the quality of a velocity model.

From the whole relocated data set, we observe that no residual rms reaches a value lower than 0.07 s (even though the PRED solution is constrained with the maximum accuracy, i.e. $Q_{EDT} = 1$, Fig. 4d), and in addition the average rms (even if much lower than in previous relocations) still extends to 0.35 s. In other words, the Q_{EDT} versus rms diagram is indicating that most probably a systematic bias affects the MAXI hypocentral determination. In the present case this bias could be attributed to (1) relatively small anomalies in the velocity model compared to the real Earth structure, that perturb the traveltimes computation, (2) the approximation done on the ray tracing computations (the shortest path method Moser 1991),

Downloaded from https://academic.oup.com/gji/article/158/2/655/771828 by guest on 01 February 2021

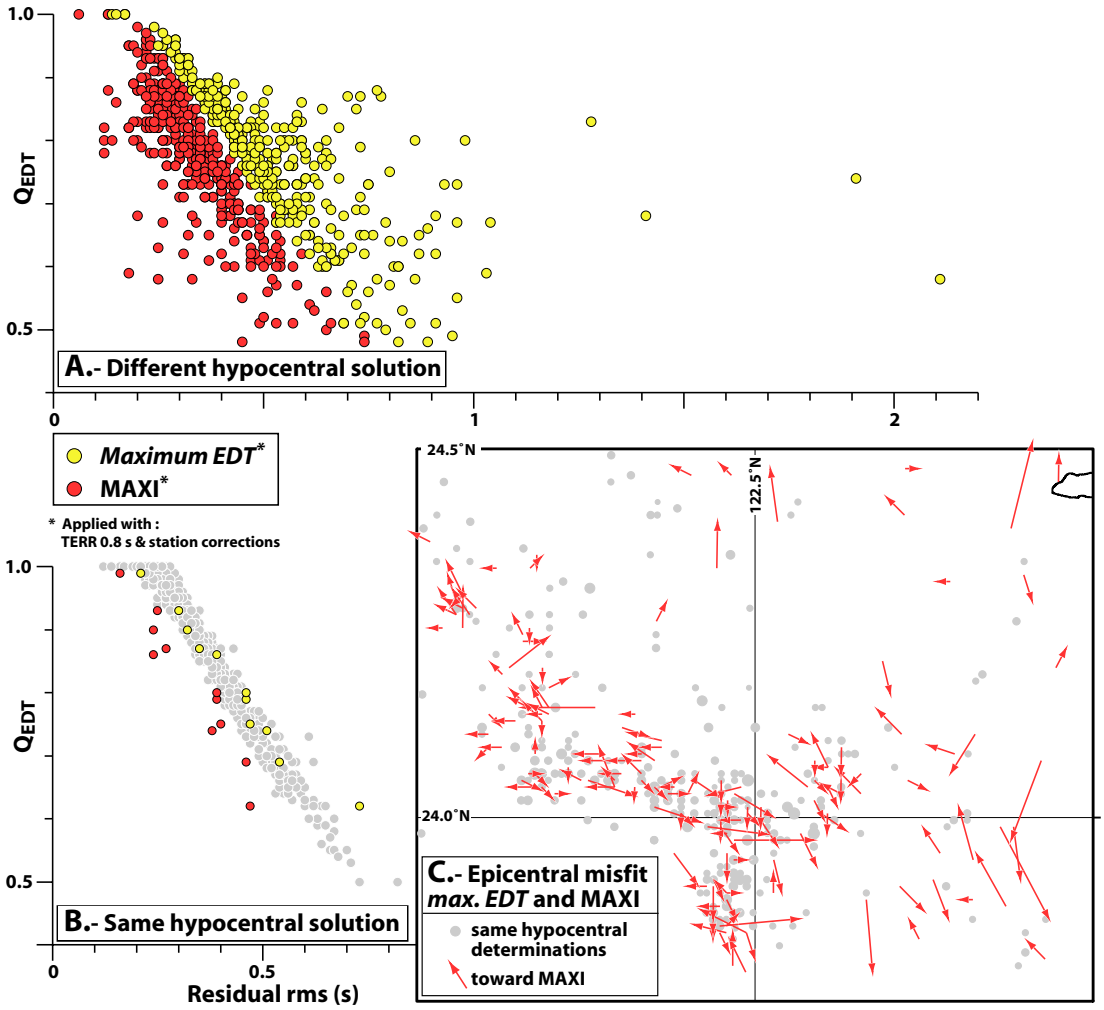

Figure 11. Comparison between maximum EDT and MAXI hypocentral determinations, both applied with TERR = 0.8 s and station corrections. (a) Q_{EDT} versus rms diagram for the earthquakes that (1) include at least one residual outlier and (2) result in a different hypocentral solution. (b) Q_{EDT} versus rms diagram for the earthquakes that present the same hypocentral solution (light grey circles correspond to earthquakes without outliers in the original data set). (c) Map view of the location difference from the maximum EDT to MAXI position.

(3) inaccuracies in the seismic data, and/or (4) the minimization process itself. At the present time the FINAL solution is constrained, in a small volume around PRED, by a grid at all points, distributed every kilometre in the horizontal and vertical directions. Imagine that the hypocentre is located exactly at the middle of the 1 km interval, generating a mislocation of 0.5 km (at maximum). If we consider an average velocity of 4 km s^{-1}, such mislocation would produce a maximal residual error of 0.215 s. Even though the residual rms error is difficult to approximate, we can easily imagine that the gridding distribution will systematically affects the relocation process. A future method for improving the algorithm could then consist in reducing the node interval implemented during the FINAL search or apply a gradient technique. Note that, in general, the cloud shape on the Q_{EDT} versus rms diagram could be analysed to assess the quality of the coherence between a seismological data set and a velocity model (e.g. to evaluate the quality of tomography model).

Using MAXI, the distribution of the distances between the PRED and FINAL position show that the minimization process results in a FINAL node that departs, on average, by 0.7 km (σ = 0.7 km), 0.9 km (σ = 0.8 km) and 1.7 km (σ = 1.2 km) from PRED along x, y and z respectively (Fig. 10b). The diminution of the distance between PRED and FINAL (compare with the maximum EDT process for the same TERR value and station correction) indicates that (1) the outlier decontamination is efficient for the minimization process, (2) the size of the search volume is well adjusted to our relocation process (i.e. the minimization is not bounded by the fixed boundaries of the search volume) and (3) the minimization process well refines the PRED location.

CONCLUSION

The new MAXI method is based on the MSM algorithm (Zhou 1994) that determine hypocentres independently. The common advantages of both methods are the following. First, they perform absolute hypocentral relocation based on arrival time measurements only. Second, they do not explicitly require the evaluation of the origin time, because the origin time is annulled through the use of EDT surfaces. Third, they can be applied even if significant lateral heterogeneities exist in the 3-D velocity model. Fourth, the residual statistics can be established efficiently by the use of a reference file (Moser 1991) that stores the ray tracing solutions. Due to the maximum combination of EDT surfaces, the computation time of

Downloaded from https://academic.oup.com/gji/article/158/2/655/771828 by guest on 01 February 2021

Table 1. Statistics for the outlier distribution per seismic station (see Fig. 8 for the spatial distribution of stations): res. aver., residual average; σ, residual standard deviation; |res| aver., average of the absolute residues; |max| and |min|, absolute larger and lower residue.

Station	No of outliers	Res. aver. (s)	σ (s)	|res| aver. (s)	|max| (s)	|min| (s)
TAP	4	−0.2	2.2	1.3	2.4	0.6
HSN	4	2.8	3.2	2.8	2.9	2.7
ILA	2	−1.0	0.5	1.0	1.0	1.0
HWA	4	2.1	12.9	2.5	5.6	0.6
CHK	4	−0.4	0.1	0.4	0.7	0.2
TTN	2	−1.4	0.4	1.4	1.4	1.4
LAY	6	−0.6	1.3	1.0	1.7	0.7
NCU	5	0.6	0.3	0.6	0.9	0.1
NST	8	1.9	3.2	1.9	3.5	0.4
ENA	3	−0.2	3.4	0.2	0.2	0.2
ESL	7	1.3	4.2	1.3	5.5	0.1
ENT	2	4.0	38.4	4.0	4.0	4.0
EHY	8	−0.9	0.9	1.2	1.8	0.8
EGS	3	1.0	6.5	1.5	2.5	0.5
NSK	1	−2.8	7.8	2.8	2.8	2.8
EHC	6	−1.0	5.6	1.3	3.4	0.3
ANP	10	2.4	2.2	2.4	4.7	0.7
TAP1	6	2.5	18.9	2.5	3.4	0.4
TWA	10	1.3	1.5	1.4	2.7	0.1
TWB1	33	−0.5	3.4	1.7	3.1	0.1
TWC	14	−0.7	1.6	1.0	3.0	0.1
TWD	1	1.5	2.3	1.5	1.5	1.5
TWE	2	−0.8	8.4	0.8	0.8	0.8
TWF1	8	−0.5	1.2	1.1	1.7	0.6
TWG	21	−0.7	2.4	1.3	4.4	0.1
TWS1	5	0.7	14.9	0.8	2.0	0.2
TWT	4	−0.5	13.7	1.7	3.3	0.8
TWU	3	−0.5	4.6	1.6	2.1	1.1
TWY	10	1.4	2.8	1.5	4.8	0.2
YON	18	−0.2	20.1	2.3	6.3	0.5
YO2	37	0.5	7.9	2.4	5.0	0.2
IRI	7	1.1	5.3	2.0	3.2	1.2
IR2	6	0.9	6.6	2.0	4.6	0.8
HAT	107	0.8	3.6	1.7	4.9	0.1
ISH	14	0.1	28.1	3.9	14.8	0.6
IS2	31	1.7	2.5	1.8	4.7	0.2
	417 ($\sigma = 18.6$)	0.4	6.7	1.7	14.8	0.1

the MAXI algorithm is increased compared with the MSM. Nevertheless, present day computational capabilities allow the MAXI algorithm to progress rapidly to a hypocentral determination.

The significant benefit of the MAXI algorithm is that it makes use of the whole seismic data set (and not only a small part) and, consequently, is able to automatically detect outliers within a set of *P* arrivals. Hypocentral *pre-determinations* are obtained robustly without any minimization process and without taking into consideration spurious measurements. In the application along eastern Taiwan, the MAXI method has significantly improved the hypocentral location for a set of data, from 1992 to 1997, located in a complex geological setting.

During this investigation, in order to inspect the capabilities of the MAXI procedure, *S* arrivals have not been implemented in the process. A detailed evaluation of the impact of EDT surfaces computed with *S* arrivals (*S*-EDT) shall be considered in the future. Because *S*-wave measurements are statistically less numerous that *P*-wave arrivals (at least, in the present study), the positive effect of *S*-EDT surfaces on the process are guaranteed only if they are incorporated at a different stage from the *P*-EDT surfaces, or if they are distinctively weighted.

Because 3-D quantitative measures of earthquake clustering (such as the entropy method suggested by Nicholson *et al.* 2000) is still very difficult to evaluate, we have approximated the improvement to hypocentral determination by comparing the relocated data with the original Taiwanese catalogue in terms of residual statistics and earthquake distribution. At the present stage of the MAXI algorithm, there is no discussion on estimating location uncertainty. To assess uncertainties as realistically as possible, a probability density function similar to the one presented by Lomax *et al.* (2000) will be implemented and result in information about the resolution of the hypocentral parameters. Alternatively, in order to evaluate as well as possible the effect of (1) the combined seismological data set (neighbouring networks), (2) the 3-D velocity model and (3) the MAXI method, it would be tempting to compare the seismological catalogues resulting from various relocation trials. This would require a proper combination of (1) Taiwanese/Taiwanese–Japanese full data sets, (2) 1-D/3-D velocity models and (3) the 'classical' and MAXI method. Each resulting catalogue would certainly vary in terms of location and only the use of synthetics would help us to really assess which solution better approximates reality. This comparison is, however, not the goal of this paper.

At the present time one of the main uncertainties of the MAXI method concerns the evaluation of the TERR parameter, i.e. the thickness given to an EDT surface. A preliminary evaluation of the seismic data is necessary to correctly evaluate the TERR value, as the dimension of TERR will influence the perception threshold of the outlier. The TERR solution used in the present version of MAXI presents a 'boxcar' shape that allows us to accept or refuse an 'outlier' at a given threshold, without any presumptions about data quality. Another solution, based on picking uncertainty, would be to use a Gaussian (or centrally peaked weighting) for the shape of the EDT surface. In future work it might be useful to find an 'adaptive' form of TERR so that the FINAL minimization step could be removed.

For now, using an appropriate boxcar TERR parameter and a single estimate of the station terms, MAXI proves to be a robust algorithm to search for earthquake locations. Because of its simple implementation (*P* arrivals and an appropriate 3-D velocity model), this method should be efficient for routine location procedures. The new hypocentre data set raises important issues regarding the tectonics at the junction between the westernmost extremity of the Ryukyu subduction and the active arc–continent collision of Taiwan; this topic shall be discussed in a later paper.

ACKNOWLEDGMENTS

The Ministry of Education of Taiwan, through the Bureau de Representation de Taipei en France, kindly provided YF with a 4-yr scholarship. This research was funded by the National Science Council to C-SL through the grants NSC85-2611-M-002-005Y, NSC86-2117-M-002a-001-ODP, NSC87-2611-M-002A-016-ODP, NSC88-2611-M-002-024-ODP and NSC89-2611-M-002-013-ODP and to HK through the grants NSC89-2921-M-001-012-EAF and NSC89-2116-M-001-017. YF also thanks the Fundació Credit Andorra for their support. Both the National Science Council and the French Institute in Taiwan support the France–Taiwan cooperation frame in Earth Sciences. Concerning the realization of the 3-D velocity model, we thank the captains, crews and technical staff of the R/V *Ocean Researcher I*, *Maurice Ewing* and *L'Atalante* for their

Downloaded from https://academic.oup.com/gji/article/158/2/655/771828 by guest on 01 February 2021

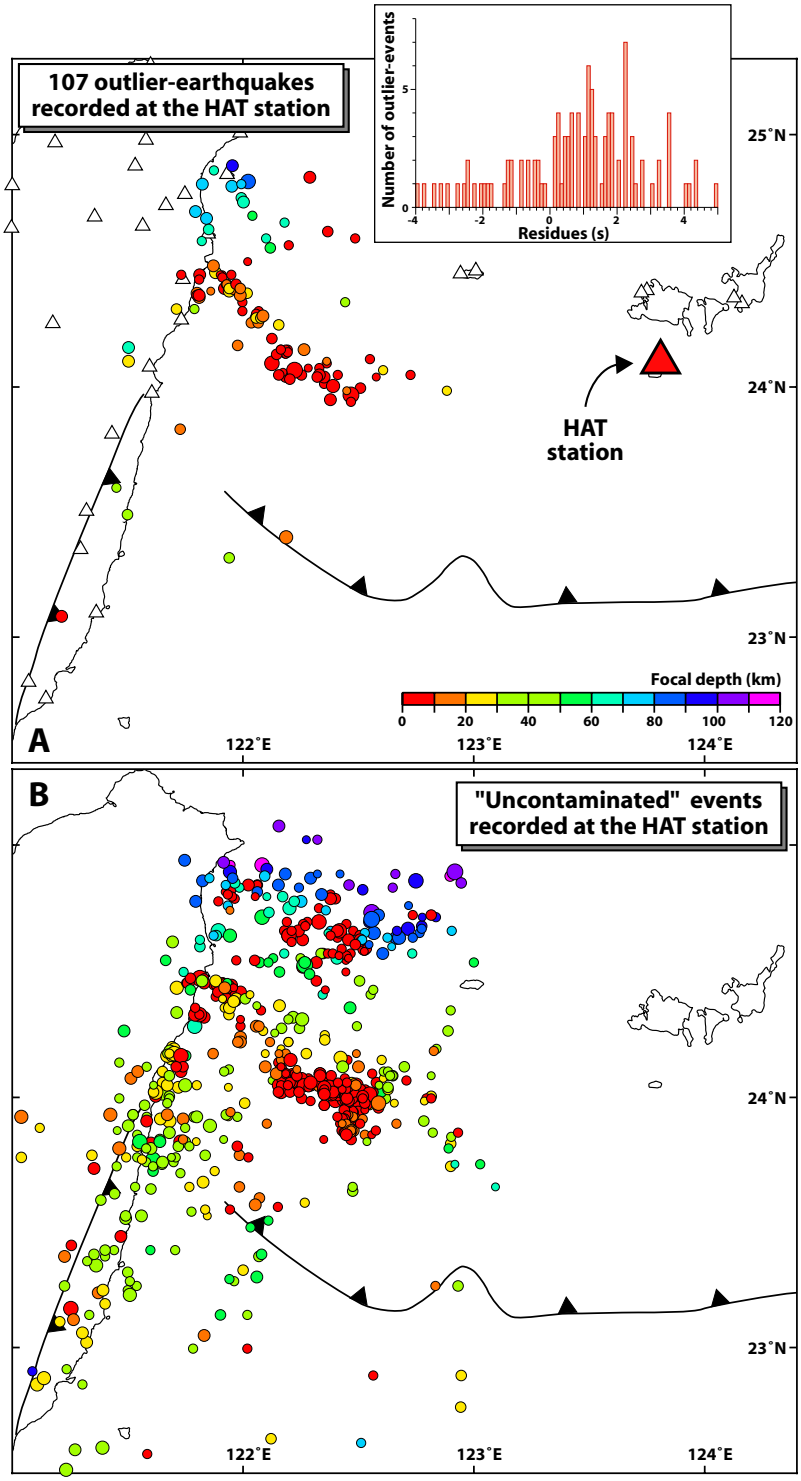

Figure 12. (a) Spatial distribution of the 107 earthquakes that contain one outlier at the HAT seismic station and associated residual histogram. Note that neither the spatial nor the residual distribution is homogeneous. (b) Spatial distribution of the remaining 664 earthquakes recorded at HAT that do not contain outliers in the original data set.

help in collecting the seismic data; Cheng Win-Bin, Chen Yen-Lin, Professor R. Shih, Eric Hetland, Hsu Shu-Kun, Kirk McIntosh, Wang Tan-Kin, Francis Wu, Yang Y.-S. shared their data and/or provided advice concerning the construction of the model. The Seismology Center of the Central Weather Bureau and Yuzo Ishikawa from the Japan Meteorological Agency are thanked for providing the earthquake data files. Zhou Hua-Wei is thanked for the algorithm code of the original MSM. Omer Gimenez is thanked for his scientific advice. Most of the figures were generated using the GMT software of Wessel & Smith (1995). We warmly thank A. Lomax and R. Willemann for their constructive reviews and M. Sambridge for his comments on entropy of earthquakes.

Downloaded from https://academic.oup.com/gji/article/158/2/655/771828 by guest on 01 February 2021

REFERENCES

Chemenda, A.I., Yang, R.-K., Hsieh, C.-H. & Groholsky, A.L., 1997. Evolutionary model for the Taiwan collision based on physical modelling, *Tectonophysics,* **274**(1–3), 253–274.

Chen, Y.-L. & Shin, T.-C., 1998. Study on the earthquake location of 3D velocity structure in the Taiwan area, *Meteorol. Bull.,* **42,** 135–169.

Cheng, W.-B., Wang, C. & Shyu, C.-T., 1996. Crustal structure of the northeastern Taiwan area from seismic refraction data and its tectonic implications, *Terr. Atmos. Ocean. Sci.,* **7**(4), 467–487.

Dominguez, S., Lallemand, S., Malavieille, J. & Schnurle, P., 1998. Oblique subduction of the Gagua Ridge beneath the Ryukyu accretionary wedge system—insight from marine observations and sandbox experiments, *Mar. Geophys. Res.,* **20**(5), 383–402.

Engdahl, E.R., Van Der Hilst, R.D. & Buland, R., 1998. Global teleseismic earthquake relocation with improved traveltimes and procedures for depth relocation, *Bull. seism. Soc. Am.,* **88,** 722–743.

Font, Y., 1996. Etude de la sismicite au nord-est de Taiwan: consequences sur la deformation de la plaque Philippine au front de la zone de collision, *Diplome d'etude approfondies thesis,* Universite de Montpellier, Montpellier, France.

Font, Y., 2001. Modes of the ongoing arc–continent collisional processes in Taiwan: new insights from seismic reflection analyses and earthquake relocation, *PhD thesis,* National Taiwan University.

Font, Y., Lallemand, S. & Angelier, J., 1999. Etude de la transition entre l'orogene actif de Taiwan et la subduction des Ryukyu—apports de la sismicite, *Bull. Soc. Geol. France,* **170**(3), 271–283.

Font, Y., Liu, C.-S., Schnurle, P. & Lallemand, S., 2001. Constraints on backstop geometry from the southwest Ryukyu subduction based on reflection seismic data, *Tectonophysics,* **333,** 135–158.

Font, Y., Kao, H., Liu, C.-S. & Chiao, L.-Y., 2003. A comprehensive 3D seismic velocity model for the eastern Taiwan–southernmost Ryukyu regions, *Terr. Atmos. Ocean. Sci.,* **14**(2), 159–182.

Got, J.-L., Fréchet, J. & Klein, F.W., 1994. Deep fault plane geometry inferred from multiplet relative relocation beneath the south flank of Kilauea, *J. geophys. Res.,* **99**(B8), 15 375–15 386.

Hagen, R.A., Duennebier, F.K. & Hsu, V., 1988. A seismic refraction study of the crustal structure in the active seismic zone east of Taiwan, *J. geophys. Res.,* **93**(5), 4785–4796.

Herrman, R.B., 1979. FASTHYPO—a hypocentre location program, *Earthquake Notes,* **50**(2), 25–38.

Hetland, E.A. & Wu, F.T., 1998. Deformation of the Philippine Sea Plate under the Coastal Range, Taiwan: results from offshore–onshore seismic experiment, *Terr. Atmos. Ocean. Sci.,* **9**(4), 363–378.

Hetland, E. & Wu, F., 2001. Crustal structure at the intersection of the Ryukyu Trench with the arc–continent collision in Taiwan: results from offshore–onshore seismic experiment, *Terr. Atmos. Ocean. Sci.,* **12,** 231–248.

Hirata, N., Kinoshita, H., Kattao, H., Baba, H., Kaiho, Y., Koresaiwa S., Ono, Y. & Hayashi, K. 1991. Report on DELP 1988 cruises in the Okinwa Trough. Part 3. Crustal structure of the southern Okinawa Trough, *Bull. Earthquake Res. Inst. Univ. Tokyo,* **66,** 37–70.

Hsu, S.-K., 2001. Subduction/collision complexities in the Taiwan–Ryukyu junction area: tectonics of the northwestern corner of the Philippine Sea Plate, *Terr. Atmos. Ocean. Sci.,* Suppl. 209–230.

Hsu, S.K. & Sibuet, J.C., 1995. Is Taiwan the result of arc–continent or arc–arc collision?, *Earth planet Sci. Lett.,* **136**(3–4), 315–324.

Jordan, T. & Sverdrup, K., 1981. Teleseismic location techniques and their application to earthquake clusters in the South-Central Pacific, *Bull. seism. Soc. Am.,* **71,** 1105–1130.

Kao, H., Shen, S.-S. & Ma, K.-F., 1998. Transition from oblique subduction to collision: earthquakes in the southernmost Ryukyu arc-Taiwan region, *J. geophys. Res.,* **103,** 7211–7229.

Kao, H., Chen, R.-V. & Chang, C.-H., 2000. Exactly where does the 1999 Chi-Chi earthquake in Taiwan nucleate?, *Terr. Atmos. Ocean. Sci.,* **11,** 567–580.

Kennett, B.L.N. & Engdahl, E.R., 1991. Travel times for global earthquake location and phase identification, *Geophys. J. Int.,* **105,** 429–465.

Lallemand, S. *et al.*, 1997a. Swath bathymetry reveals active arc–continent collision near Taiwan, *EOS, Trans. Am. geophys. Un.,* **78**(17), 173–175.

Lallemand, S., Liu, C.-S. & Font, Y., 1997b. A tear fault boundary between the Taiwan orogen and the Ryukyu subduction zone, *Tectonophysics,* **274**(1–3), 171–190.

Lallemand, S., Liu, C.S., Dominguez, S., Schnurle, P., Malavieille, J. & the ACT scientific crew 1999. Trench-parallel stretching and folding of forearc basins and lateral migration of the accretionary wedge in the southern Ryukyus: A case of strain partition caused by oblique convergence, *Tectonics,* **18**(2), 231–247.

Lee, W.H.K. & Lahr, J.C., 1975. HYPO71 (revised): a computer program for determining hypocenter, magnitude, and first pattern of local earthquakes, *US Geological Survey Open-File Report 75–311,* pp. 1–116.

Lomax, A., Virieux, J., Volant, P. & Berge, C., 2000. Probabilistic earthquake location in 3D and layered models: introduction of a Metropolis–Gibbs method and comparison with linear locations, in, *Advances in Seismic Event Location,* pp. 101–134, eds Thurber, C. & Rabinowitz, N., Kluwer, Amsterdam.

McIntosh, K. & Nakamura, Y., 1998. Crustal structure beneath the Nanao forearc basin from TAICRUST MCS/OBS Line 14, *Terr. Atmos. Ocean. Sci.,* **9**(3), 345–362.

McIntosh, K. & Nakamura, Y., 1999. Structure and tectonics offshore south and east of Taiwan: some results of the TAICRUST MCS/OBS survey, *SEASIA Conference,* Mem. Geosci. Montpellier, May 1999, Montpellier, p. 261.

Moser, T.J., 1991. Shortest path calculation of seismic rays, *Geophysics,* **56,** 59–67.

Moser, T.J., Van Eck, T. & Nolet, J., 1992. Hypocenter determination in strongly heterogeneous Earth models using the shortest path method, *J. geophys. Res.,* **97,** 6563–6572.

Nicolson, T., Sambridge, M. & Gudmundsson, O., 2000. On entropy and clustering in earthquake hypocenter distributions, *Geophys. J. Int.,* **142,** 37–51.

Pavlis, G.L. & Booker, J.R., 1980. The mixed discrete–continuous inversion problem: application to the simultaneous determination of earthquake hypocenters and velocity structure, *J. geophys. Res.,* **85,** 4801–4810.

Poupinet, G., Ellsworth, W.L. & Frechet, J., 1984. Monitoring velocity variations in the crust using earthquake doublets: an application to Calaveras Fault, California, *J. geophys. Res.,* **89,** 5719–5731.

Pujol, J., 1988. Comments on the joint determination of hypocenters and station corrections, *Bull. seism. Soc. Am.,* **78,** 1179–1189.

Pujol, J., 1992. The relationship between JHD and 3D velocity inversion, *Seismol. Res. Lett.,* **63,** 57.

Pujol, J., 1995. Application of the JHD technique to the Loma Prieta, California, mainshock–aftershock sequence and implication for earthquake location, *Bull. seism. Soc. Am.,* **85**(1), 129–150.

Rau, R.-J. & Wu, F.T., 1995. Tomographic imaging of lithospheric structures under Taiwan, *Earth. planet. Sci. Lett.,* **133,** 517–532.

Rubin, A.M. & Gillard, D., 2000. Aftershock asymmetry/rupture directivity among central San Andreas fault microearthquakes, *J. geophys. Res.,* **105**(B8), 19 095–19 109.

Schnurle, P., Liu, C.-S., Lallemand, S. & Reed, D., 1998a. Structural controls of the Taitung Canyon in the Huatung basin east of Taiwan, *Terr. Atmos. Ocean. Sci.,* **9**(3), 453–472.

Schnurle, P., Liu, C.-S., Lallemand, S. & Reed, D., 1998b. Structural insight into the south Ryukyu margin: effects of the subducting Gagua Ridge, *Tectonophysics,* **288,** 237–250.

Sibuet, J.-C. & Hsu, S.-K., 1997. Geodynamics of Taiwan arc–arc collision, *Tectonophysics,* **274,** 221–251.

Smith, E., 1982. An efficient algorithm for routine joint hypocenter determination, *Phys. Earth planet. Inter.,* **30,** 135–144.

Thurber, C.H., 1983. Earthquake locations and three-dimensional crustal structure in the Coyote Lake area, central California, *J. geophys. Res.,* **88,** 8226–8236.

Waldhausser, F. & Ellsworth, W.L., 2000. A double-difference earthquake location algorithm: method and application to the Northern Hayward Fault, California, *Bull. seism. Soc. Am.,* **90**(6), 1353–1368.

Downloaded from https://academic.oup.com/gji/article/158/2/655/771828 by guest on 01 February 2021

Wang, T.-K. & Chiang, C.-H., 1998. Imaging of arc-arc collision in the Ryukyu forearc region offshore Hualien from TAICRUST OBS line 16, *Terr. Atmos. Ocean. Sci.,* **9**(3), 329–344.

Wang, T.-K. & Pan, C.-H., 2001. Crustal Poisson's ratio off Eastern Taiwan from OBS data modeling, *Terr. Atmos. Ocean. Sci.,* **12,** 249–269.

Wessel, P. & Smith, W.H.F., 1995. New version of the Generic Mapping Tools released, *EOS, Trans. Am. geophys. Un.,* **76,** 329.

Wittlinger, G., Herquel, G. & Nakache, T., 1993. Earthquake location in strongly heterogenous media, *Geophys. J. Int.,* **115,** 759–777.

Yang, Y.-S., 1999. Crustal velocities of the Huatung Basin from refracted and reflected data, *Masters thesis*, National Taiwan Ocean University, Keelung (in Chinese).

Yang, Y.-S. & Wang, T.-K., 1998. Crustal velocity variation of the western Philippine Sea Plate from TAICRUST OBS/MCS Line 23, *Terr. Atmos. Ocean. Sci.,* **9**(3), 379–393.

Yu, S.-B., Chen, H.-Y. & Kuo, L.-C., 1997. Velocity field of GPS stations in the Taiwan area, *Tectonophysics,* **274,** 41–59.

Zhou, H.-W., 1994. Rapid three-dimensional hypocentral determination using a master station method, *J. geophys. Res.,* **99**(B8), 15 439–15 455.

Downloaded from https://academic.oup.com/gji/article/158/2/655/771828 by guest on 01 February 2021